A Deep *Chandra* X-Ray Observation of the Rich Young Cluster NGC 6530. I: The X-Ray Source Catalog and the Cluster Population

F. Damiani, E. Flaccomio, G. Micela, S. Sciortino

INAF - Osservatorio Astronomico di Palermo G.S.Vaiana, Piazza del Parlamento 1, I-90134 Palermo, ITALY

damiani@oapa.astropa.unipa.it, ettoref@oapa.astropa.unipa.it, giusi@oapa.astropa.unipa.it, sciorti@oapa.astropa.unipa.it

and

F. R. Harnden Jr., S. S. Murray

Smithsonian Astrophysical Observatory, 60 Garden Street, Cambridge, MA 02138

ABSTRACT

In a deep 60 ks *Chandra* ACIS X-ray observation of the very young cluster NGC 6530 we detect 884 point X-ray sources and argue that a very large fraction of them (90-95%) must be pre-main-sequence cluster members, mostly of low masses. This is a significant enlargement of the known NGC 6530 stellar population with respect to previous optical studies, including Hα surveys. We identify 220 X-ray sources with catalogued stars down to $V = 17$, while most unidentified sources have fainter counterparts. Moreover, we find an infrared counterpart in the 2MASS catalog for 731 X-ray sources. The optically identified cluster X-ray sources are found in a band in the H-R diagram above the main sequence, in the locus of 0.5-1.5 Myr PMS stars, with masses down to 0.5-1.5 $M_\odot$. We find evidence of an age gradient across the field from northwest to south, suggesting a sequence of star formation events qualitatively similar to that found in earlier studies of the same region, but differing in the details. A group of X-ray sources showing frequent flares may be associated with the youngest stars in the cluster, suggesting that X-ray flaring activity is especially intense in the youngest PMS phases of low-mass stars.

Subject headings: open clusters and associations: individual (NGC 6530) — stars: coronae — stars: pre-main-sequence — X-rays: stars

1. Introduction

NGC 6530 is a very young cluster closely associated with the M8 nebula. This emission nebula is excited primarily by bright nearby O stars: the extremely young object Herschel 36 (O7 V), which illuminates the brightest part of M8 (the "Hourglass Nebula"), 9 Sgr (O4 V) and HD 165052 (an O6.5 V + O6.5 V binary). In addition to O stars, NGC 6530 contains about 60 B stars (Sung, Chun and Bessell 2000, hereafter SCB), making it $\sim 3 - 4$ times richer in massive stars than the Orion Nebula Cluster. NGC 6530 is much farther away than the Orion Nebula: its distance has recently been estimated to be $d = 1.8$ kpc (SCB), while earlier estimates were in the range $d = 1.3 - 2.0$ kpc (Thé 1960, Walker 1957). The NGC 6530 age was estimated as $\sim 1.5 - 2.0$ Myr (van Altena and Jones 1972, Sagar and Joshi 1978, SCB), slightly older than the Orion Nebula Cluster (Hillenbrand 1997).

The M8 emission nebula is the illuminated, nearest part of a giant molecular cloud, along the same line of sight as the visible NGC 6530 cluster, in which some of its members may be still embedded. The thick, dense molecular cloud is visible in optical images, since its non-excited parts are dark and absorb the light of background stars. The nearly complete absence of background stars can also be verified from the HR diagram of the cluster region (see e.g., that shown in SCB), which shows essentially no stars fainter than the main sequence at the cluster distance, for a given color.

NGC 6530 has been the subject of a number of optical studies, both to investigate its massive stars and to search for lower-mass stars. Low-mass stars coeval to massive OB stars are expected to be still in their pre-main-sequence (PMS) evolutionary stages, falling above the main sequence in the cluster HR diagram. Walker (1957) found indications of a band of less massive stars above the main-sequence and tentatively identified these stars as contracting PMS stars. Later, Thé (1960) and Chini and Neckel (1981) found that this result was not statistically significant when compared to the local density of field stars. A proper-motion study was then made by van Altena and Jones (1972), but in excluding stars fainter than $V \sim 13.6$, they missed most of the stars hypothesized by Walker to be in the PMS stage. The existence of a PMS stellar population has therefore remained controversial until very recently. An optical study by SCB yielded only 37 (plus 9 candidate) low-mass PMS members, selected through their bright Hα emission (typical of classical T Tauri stars); since many low-mass PMS stars exist without Hα emission this low-mass PMS sample under-represents the true low-mass PMS cluster population. Focused mainly on the massive stars, instead, were the photometric studies by Kilambi (1977) and Sagar and Joshi (1978), and the photometric/spectroscopic study by van den Ancker et al. (1997).

NGC 6530 and M8 have also attracted attention because they provide hints of a "sequential" star-formation process (Lada et al. 1976), in which the NGC 6530 cluster formed first, and Herschel 36, embedded in the Hourglass Nebula about 5 pc to the west of NGC 6530, formed much more recently. Tothill et al. (2002) have studied this region at sub-mm and mm-wavelengths, and have found strings of cloud cores, which may be induced to collapse and form stars under the action of the external pressure/shock front.

The current lack of knowledge on the bulk of the NGC 6530 stellar population has motivated us to perform an X-ray study of this cluster with the *Chandra* X-ray Observatory (Weisskopf et al. 2002). It is well known that PMS stars have strong X-ray emission and clearly stand out in X-ray images compared to older, X-ray fainter field stars, thus enabling an accurate and efficient selection of low-mass cluster members.

M8 was recently observed in X-rays with XMM-Newton (Rauw et al. 2002). This observation was targeted at the Hourglass/Herschel 36 region, and only part of NGC 6530 falls in its field of view. Unlike these *Chandra* data, moreover, the XMM-Newton data have insufficient spatial resolution to fully resolve the dense cluster of X-ray sources. An archival ROSAT/PSPC observation (unpublished) shows distinct X-ray sources associated with 9 Sgr and Herschel 36, but only unresolved emission ($\sim 10'$ wide) coincident with the NGC 6530 center.

We present our new *Chandra* X-ray data in Section 2. In § 3 we deal with the optical identification of detected X-ray sources. § 4 contains a discussion of our results on the cluster population. A few more general conclusions on the cluster are discussed in § 5, and § 6 provides a summary of our results. The study of the ACIS X-ray spectra of NGC 6530 sources, and the analysis of the properties of the X-ray emission are presented in a companion paper (Damiani et al., in preparation, hereafter Paper II).

2. The X-ray Observation and Data Reduction

NGC 6530 was observed for 60 ks with the *Chandra* ACIS-I CCD detector (Townsley et al. 2000) on June 18-19, 2001, as part of the GTO program. The ACIS-I field of view (FOV) is square, $16.9' \times 16.9'$ on the sky (only chips 0-3 are used). The pointing direction (R.A. 18:04:24.38, Decl. –24:21:05.8) was chosen coincident with the NGC 6530 cluster center, and because of the limited FOV we could not observe the Hourglass/Herschel 36 region, located $\sim 10'$ from cluster center. Figure 1 shows a Digital Sky Survey (second epoch) red image of NGC 6530, with overlaid the ACIS-I FOV, and the positions of X-ray detected sources (see below).

ACIS-I images have a very narrow point-spread function (PSF; FWHM $\sim 0.5''$ on-axis). X-ray photons are accumulated and read out every 3.2 s, so that timing analysis of not too intense sources can be made. The ACIS has moderate spectral resolution (R$\sim 35-50$ around 1 keV), allowing a spectral analysis to be performed.

We have inspected the ACIS background light curve, to check whether high-background time intervals were present, as a consequence of eruptive solar activity. High-background episodes are capable of significantly deteriorating the data quality and must be screened out to achieve the best sensitivity for detecting sources. Fortunately, no such high-background intervals occurred during the NGC 6530 observation, and we therefore did not have to apply time filtering. As a consequence, we are able to study X-ray light curves of detected X-ray sources over an uninterrupted time span of 60 ks.

We have processed the raw X-ray event file using CIAO[1] to apply Charge-Transfer Inefficiency correction and correct for "afterglow" spurious events. We selected (standard) event grades 0,2,3,4,6, and selected only photons in the energy range 0.3-8.0 keV. The ACIS image so obtained is shown in Figure 2 and reveals a crowded cluster of hundreds point X-ray sources, nevertheless it not confused thanks to *Chandra's* superb resolution. A zoom of the dense central region of this field is shown in Figure 3. The large number of point sources puts this cluster in a class with *Chandra* images of other massive star-formation regions, such as the Orion Nebula, M17 and M16.

Source detection was performed using a l keV exposure map with *Pwdetect*[2], a wavelet-based source detection algorithm developed at the Osservatorio Astronomico di Palermo on the basis of its ROSAT predecessor *wdetect* (Damiani et al. 1997a,b) and previously employed on *Chandra* data by Harnden et al. (2001), Flaccomio et al. (2003), and Damiani et al. (2003), where a brief account of its features can be found. *Pwdetect* found 884 point X-ray sources in the NGC 6530 ACIS-I image, with a significance threshold chosen to ensure only one spurious detection on average. The narrow PSF and extremely low background (≤ 0.1 counts/square arcsec on-axis) of *Chandra* permit confident detection of sources with as few as 4 or 5 X-ray counts within $5'$ of field center, and with 15 to 25 counts in the outermost field regions. Detected source count rates were measured using *Pwdetect* as well. The list of detected X-ray sources in NGC 6530 is reported in Table 1. In this Table we also report the probability that the X-ray source is constant according to a Kolmogorov-Smirnov test (column P_{KS}), and two hardness ratios (columns HR1 and HR2), each defined as $(H-S)/(H+S)$, where H and S are the source counts in two energy bands, here chosen as [0.75-1.5] and [0.3-0.75] keV for HR1, and [1.5-8.0] and [0.75-1.5] keV for HR2.

---

[1]Version 2.3: http://cxc.harvard.edu/ciao

[2]*Pwdetect* is available publicly at the address:
http://www.astropa.unipa.it/progetti_ricerca/PWDetect/

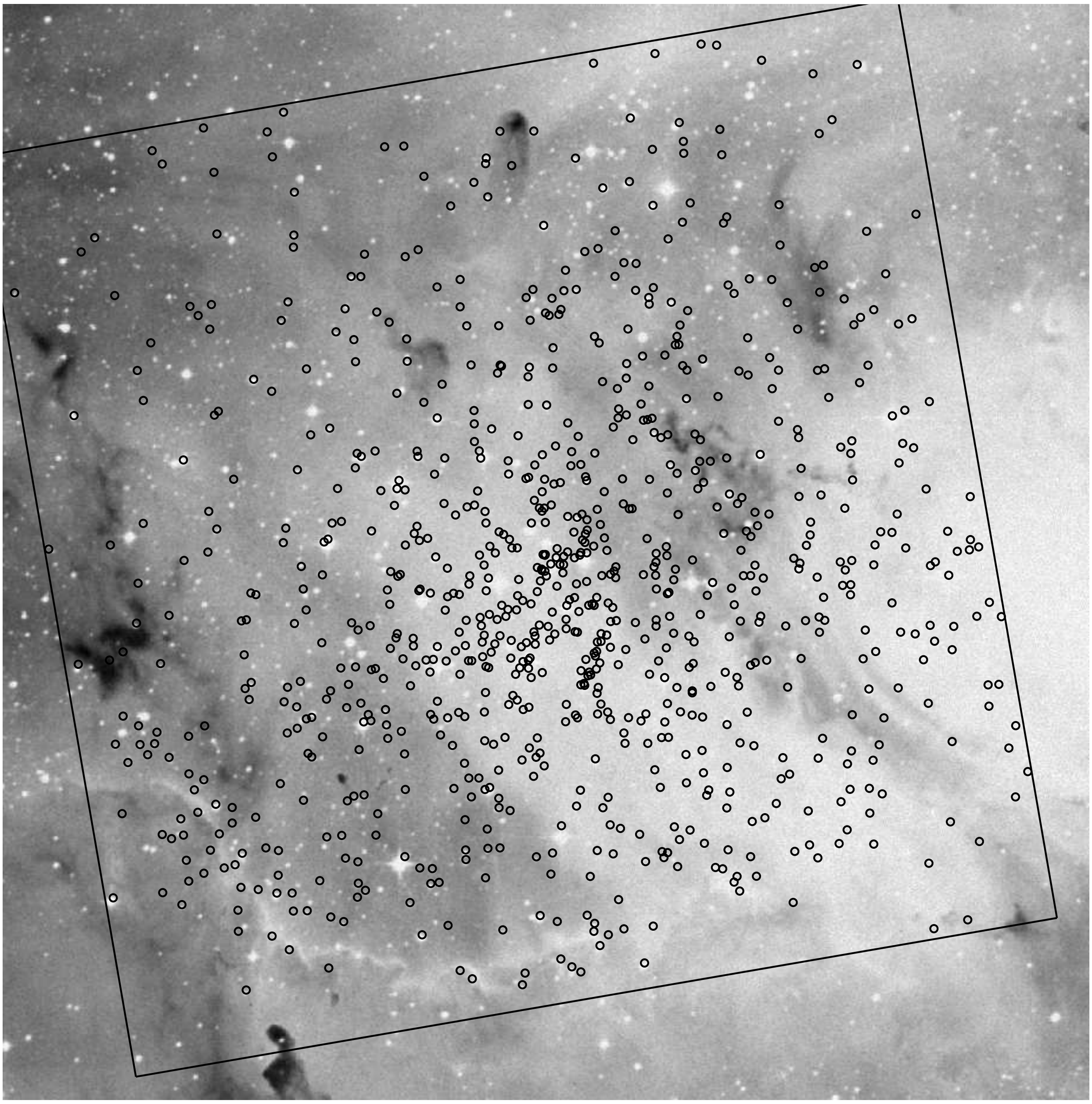

Fig. 1.— DSS red image of NGC 6530 and M8, with overlaid the ACIS-I field of view. The brightest part of the nebula, the so-called Hourglass Nebula, and its illuminating star Herschel 36, lie just outside the ACIS field. Detected X-ray sources are indicated by small circles. The ACIS-I FOV is 16.9′ on a side. North is up and east is to the left.

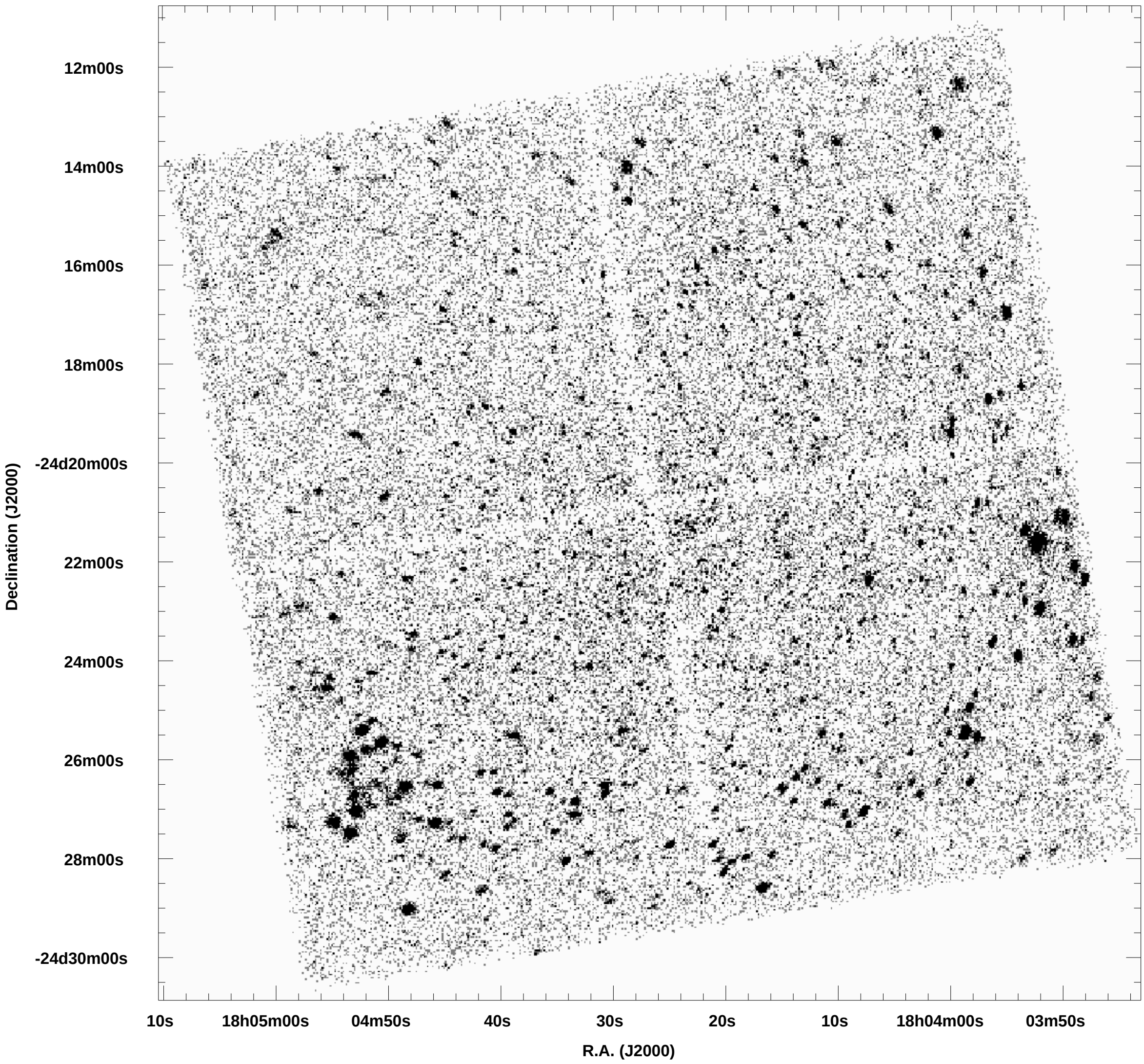

Fig. 2.— ACIS-I X-ray image of NGC 6530, in the band 0.5–8.0 keV. 884 point X-ray sources are detected. North is up and east is to the left.

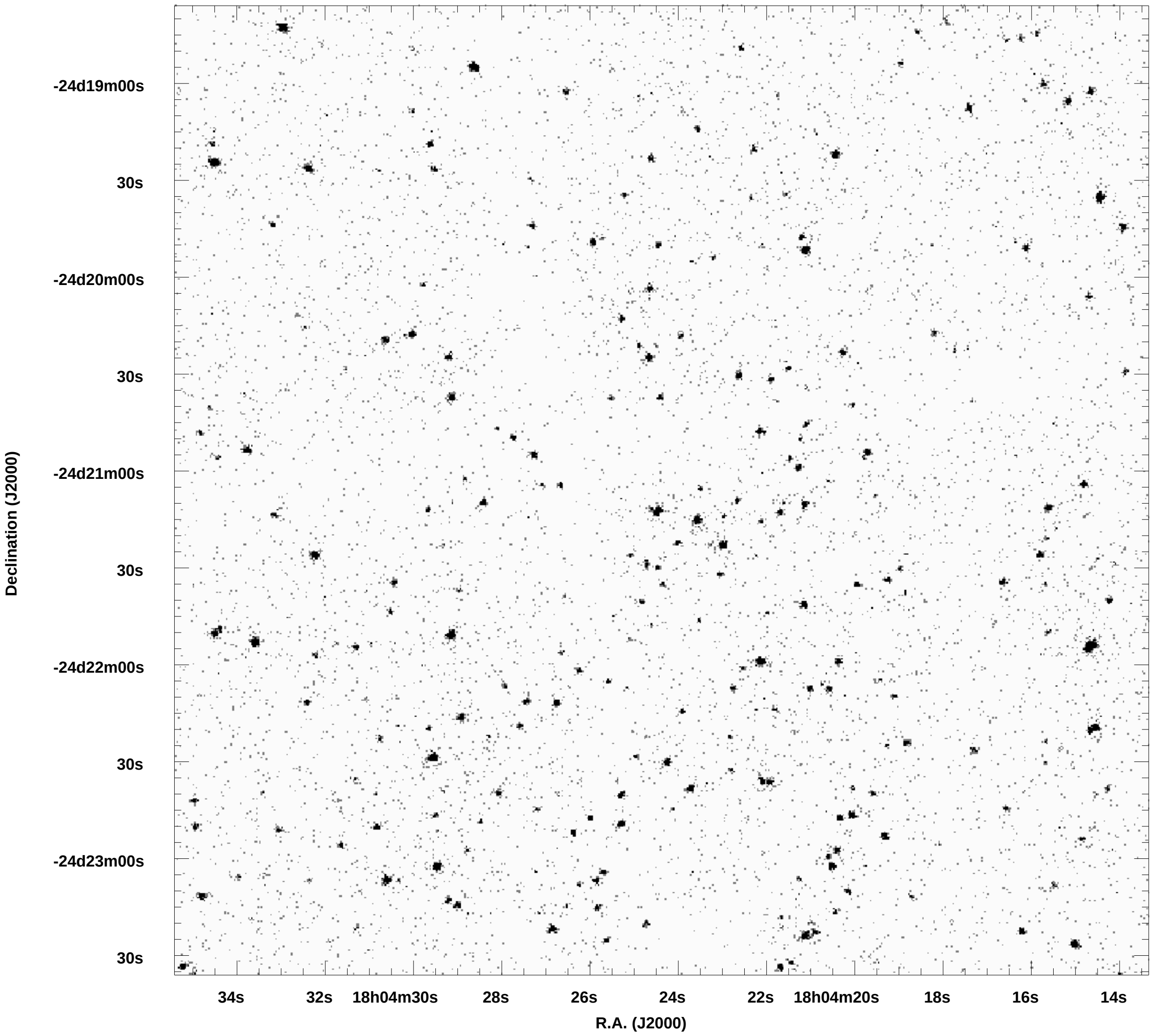

Fig. 3.— Full-resolution zoom of central $5' \times 5'$ of the ACIS image, where spatial resolution is highest, corresponding to NGC 6530 cluster center.

3. Optical-Infrared Data and X-Ray Sources Identification

3.1. Available Data

Optical data on stars in the NGC 6530 region were taken from the previous works noted in §1, in particular from the recent work by SCB. This latter study had the deepest limiting magnitude (complete to $V = 17$ with a few stars fainter than this limit) and hence contains the largest number of stars. SCB reports V magnitudes, $U - B$, $B - V$, $V - I$ color indices, and an $R - H\alpha$ index as a measure of Hα emission relative to the nearby continuum (analogous to the line equivalent width). Spectral types are available (from the SIMBAD database) for only 68 stars in the ACIS FOV, most having $V \leq 13$). For all other stars, the spectral type was estimated from their $B - V$ and $V - I$ colors, as in Damiani et al. (2003; their Table 7). Because of its $V = 17$ magnitude limit, only a few stars in the SCB catalog have optical colors of M stars.

As remarked in § 1, a consolidated member list is not available for stars later than about type A0, which are expected to be still contracting towards the main sequence. The proper-motion study by van Altena and Jones (1972) was complete only down to $V \sim 13.6$, corresponding to mid-A on the main sequence. Using the $R - H\alpha$ index, SCB have selected 37 low-mass PMS members of NGC 6530, plus 9 candidate members, mostly in the range $V = 14.5 - 18.0$. Since the SCB selection probably misses many cluster members already present in their catalogue, we have cross-correlated our X-ray source catalog not with an optical list of members, but with the whole SCB catalog. There are 611 SCB stars falling in our ACIS FOV.

The SCB survey does not cover the easternmost $2.25'$ of the ACIS FOV (R.A. later than 18:04:52) comprising about 13% of the FOV. There are 46 detected X-ray sources (5.2% of total) in the area not covered by SCB. The percentage of these latter sources is smaller than the uncovered area percentage because the NGC 6530 X-ray source are strongly clustered around the center, as discussed in §4.3.

We have also taken advantage of the availability of the 2MASS All-Sky Catalog of near-IR sources. We found 9112 2MASS sources falling in the ACIS FOV. However, following the 2MASS Explanatory Supplement (Cutri et al. 2003), we have selected only those sources unaffected by strong photometric uncertainties, discarding detections with *ph_qual*=*'E'*, *'F'*, *'U'* or *'X'*, or with *cc_flg*=*'p'*, *'d'* or *'s'*. We have anyway retained sources with some confusion-related problems (*cc_flg*=*'b'* or *'c'*), a significant fraction of the total in such a crowded region. This selection results in 8792 good 2MASS sources. The number of 2MASS sources in the ACIS FOV is therefore much larger than the number of SCB stars, and moreover IR sources are less affected by extinction, and can be used to probe stars embedded in the cloud or behind it.

One further advantage of using the 2MASS catalog lies in its good astrometric accuracy (80-100 mas with respect to Tycho-2 catalog; Cutri et al. 2003). Therefore, we have matched positions of SCB stars with 2MASS sources, and after correcting for shifts of $0.7''$ in R.A., and $-0.09''$ in Decl., we have found 851 SCB-2MASS identifications within $1.3''$ (of which 583 in the ACIS FOV). Five cases of double identifications within this distance turned into single identifications by using a smaller matching distance of $0.6''$, thus obtaining a list of unique identifications.

3.2. 2MASS–X-ray Source Identification

Since the 2MASS sample in our ACIS FOV is larger than the SCB sample, and gives more accurate positions, we have first matched positions of our X-ray sources with 2MASS sources. We have used a matching distance $d < 4\sigma_X$ (where σ_X is the *Pwdetect* X-ray position error). In doing this, we found and corrected a systematic X-ray position shift of $0.3''$ in R.A., and $1.75''$ in Decl. (thus obtaining more accurate X-ray positions, reported in Table 1). For three X-ray sources with such a small X-ray error that $4\sigma_X$ was less than $1.5''$, we relaxed the identification condition to $d < 1.5''$. This resulted in a number of multiple identifications, among which four turned into single by using a reduced distance $d < 1.5\sigma_X$. This leaves us with 13 double and 2 triple X-ray-2MASS identifications. The total number of X-ray sources with 2MASS counterpart(s) is 731, reported in Table 1. The agreement between X-ray and 2MASS positions is excellent in most cases, with offsets below $1''$.

From the total cross-identification area and the 2MASS source density we may expect 215 spurious identifications, more than one quarter of the total. Since however we expect indeed a strong real correlation between our X-ray and 2MASS samples, this number is probably unrealistically large. We have therefore derived it differently. We expect the tail of the offset distribution to be more affected by spurious identifications than the distribution peak. Therefore, we counted 21 X-ray sources with identification between $3 - 4\sigma$, of which a significant fraction may be spurious. In particular, if we have overestimated our X-ray position error, nearly all of these 21 may be spurious identifications. Since, based on simple geometrical arguments, the number of spurious identifications in the range $3 - 4\sigma$ is 43.75% of all spurious identifications within 4σ, we would obtain a maximum total number of 48 spurious identifications in our sample. If instead our X-ray position error is correct, we expect 1.08% of all real identification to fall in the $3 - 4\sigma$ range (in two dimensions, offsets are distributed as $P(r)dr = \exp(-r^2/2)rdr$, with r in units of σ), and thus among the 21 identifications in this range, 8 will be real and 13 spurious, from which one derives a total number of 30 expected spurious identifications. To summarize, we conclude that the plausible number of spurious X-ray-2MASS identifications is between 30 and 50.

3.3. Optical–X-ray Source Identification

We then performed a cross-correlation of our X-ray positions with the optical star positions of SCB, using a matching distance $d < 4\sigma_X$ (where σ_X is the *Pwdetect* X-ray position error). In doing this, we applied a systematic shift between X-ray- and SCB positions, computed from the shifts already found, of $-0.4''$ in R.A., and $1.84''$ in Decl. For one X-ray source with such a small X-ray error that $4\sigma_X$ was less than $2''$, we relaxed the identification condition to $d < 2''$. The agreement between X-ray and optical positions is again very good (cf. Table 1). In this case we find no ambiguous identifications, mostly because of the much smaller size of the SCB sample (limited to $V \leq 17$) compared to the 2MASS sample. In addition to the O7 star 9 Sgr, not listed by SCB but identified with the brightest X-ray source (# 22) in the ACIS FOV, we uniquely identify 219 X-ray sources, each with a SCB optical star. Optical counterparts for the remaining 664 unidentified X-ray sources (excluding 46 sources outside the SCB surveyed region) are either fainter than $V = 17$ or are found in regions with bright nebulosity or nearby bright stars. We have also computed *Pwdetect* count-rate upper limits for 391 other SCB stars which fell in the ACIS FOV but were not detected. Overall, there remain 146 X-ray sources with no optical nor IR identification.

We estimate that as many as 28 of our 220 optical identifications may by spurious, with these found preferentially in the outer parts of the FOV where the ACIS PSF, positional errors and the matching distances are larger. This number is derived under the assumption that the X-ray and optical populations are uncorrelated, probably not the case for most objects in the NGC 6530 field. Analogously to the case of 2MASS identifications, it therefore should be regarded as an overestimate.

4. The NGC 6530 Cluster Stellar Population

4.1. Non-Member Contamination

The number of X-ray sources we detect in the NGC 6530 ACIS field is so large that it leaves little doubt that most of them are indeed cluster members. Here we try to estimate more quantitatively the number of "contaminating" X-ray sources, which do not belong to the cluster but are either foreground or background objects. To this aim we have searched the *Chandra* data archive for other pointings toward nearby sky regions (especially at nearly the same galactic latitude), with the same detector and with at least as long exposure time, to be used as a "control field" for the field-object X-ray sources. There are not many archived observations meeting these requirements, and the best candidate we found is a 58 ks ACIS observation of the Galactic Plane (ObsId 1523), pointed at galactic coordinates $l = 28.45$, $b = -0.2$ degrees (our NGC 6530 field is at $l = 6.08$, $b = -1.31$ degrees). In this field *Pwdetect* detected 119 point X-ray sources (in addition to a few possible diffuse sources). This is a significantly smaller number than that detected in NGC 6530. Figure 4 shows the detected count-rate distributions for NGC 6530 (white bars) and this Galactic Plane pointing (grey bars). If the number and types of field X-ray sources are the same for the Galactic Plane field and NGC 6530, then most of the expected contamination occurs at the lowest X-ray fluxes, while virtually no contamination is present for count rates larger than 10^{-3} counts/s. Moreover, we have found that most of the Galactic Plane X-ray sources have hard X-ray spectra (although only a handful of counts are detected for most of them), namely harder than those of most NGC 6530 sources. Ebisawa et al. (2001) have studied this Galactic Plane pointing and concluded that most of these point sources are probably extragalactic objects seen through the galactic disk, i.e., preferentially background rather than foreground objects.

Because NGC 6530 lies in front of a dense, opaque dust cloud (cf. § 1), the total galactic absorption in this direction is much larger than the simple galactic-plane value. Therefore, any background objects would be detected with still lower fluxes than those in the Galactic Plane pointing. Moreover, they will be found preferentially among the hardest X-ray sources detected. Hence we estimate that the number of unrelated field objects that we detect as X-ray sources in the NGC 6530 field is definitely not larger than 120, and more probably of order of ~ 50 objects, most of which would have very low count rates.

We plot also in Figure 4 the count-rate distribution of NGC 6530 X-ray sources which are identified with optical stars. These are more frequent at higher count rates, where the fraction of expected contaminants decreases. If we consider only optically identified X-ray sources, the number of expected detected non-members (computed as $\sum_i N_i^{GalPl} N_i^{ident}/N_i^{tot}$, where the sum runs over count-rate bins, and N^{GalPl}, N^{tot} and N^{ident} are the numbers of detections in the Galactic Plane field, the total number of detections in NGC 6530, and the optically identified sources in NGC 6530, respectively) drops to 17 at most, and is probably much lower. We conclude therefore that at least 90% of the X-ray sources detected in NGC 6530 are very probable cluster members, and this percentage rises to 95% considering only sources with optical counterparts in the SCB catalog.

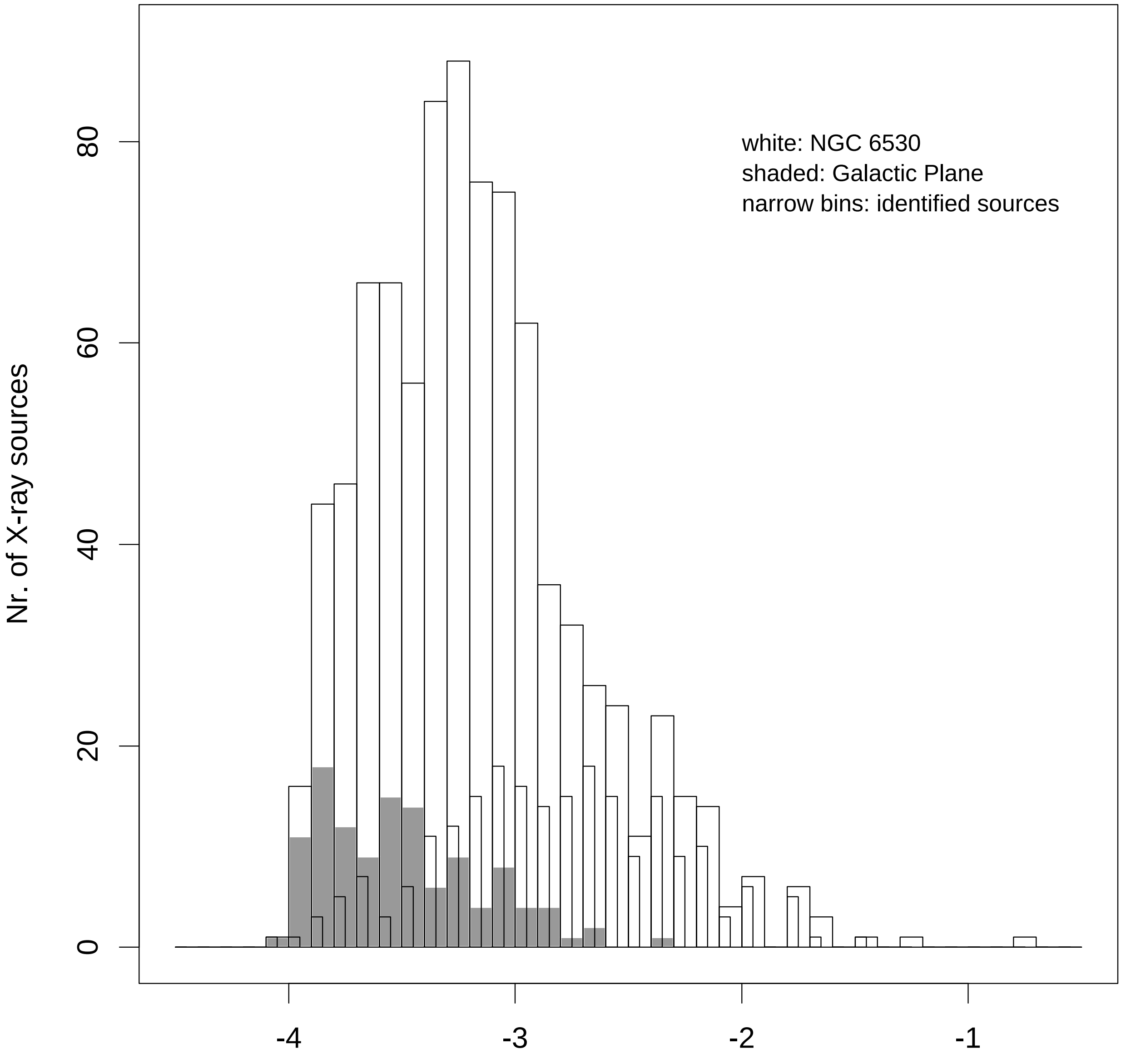

Fig. 4.— Histograms of detected source count rates in the NGC 6530 field (white), and in a reference galactic-plane field with the same sensitivity (shaded). The narrow bins indicate the count-rate distribution for optically identified sources.

4.2. Background/Embedded Stars from 2MASS Data

Using 2MASS IR data we have tried to obtain more clues about the nature of objects falling in the ACIS FOV, and in particular of detected X-ray sources. Figure 5*a* shows a $(H-K, J-K)$ color-color diagram for all 2MASS sources in the ACIS FOV with a valid detection in the J, H, and K bands (small dots), with crosses indicating X-ray detected sources. Also shown are the reddened 1-Myr isochrone between 0.16-7 $M_{\odot}$ (see § 4.5; in this diagram, it is very similar to the ZAMS), and the reddening vector (from Rieke and Lebofsky 1985). Figure 5*b* is an analogous diagram including only SCB stars in the FOV. Figure 5*a* shows that most 2MASS sources in the field are found distributed in a strip, nearly parallel to the extinction vector, up to $H-K \sim 1.7$. The largest $H-K$ for stars with $A_V \sim 1$ is about 0.4, and therefore the much larger values of $H-K$ found are indicative of high reddening ($A_V \sim 5-15$ for most sources, and ranging up to $A_V \sim 30$). Only about 60 among these high-reddening 2MASS sources are X-ray detected, well compatible with the expected number of background X-ray sources (§ 4.1). Most X-ray detections are instead found along the 1-Myr cluster isochrone, indicating low-reddening, normal photospheric emission. Some X-ray sources show redder IR colors, but not along the reddening vector, suggesting possible IR excesses from circumstellar dust.

Figure 5*b* contains only SCB stars (with $V<17$), and we may see that while the pattern of X-ray detected sources has not basically changed, the strip of heavily absorbed sources has almost disappeared. In particular, there are no more X-ray detected, high-extinction sources. Therefore, while among IR-identified X-ray sources we find a few tens of sources with $A_V \sim 5-15$, virtually no such high extinction is found among optically identified X-ray sources (within the SCB limit). In either case, most X-ray sources are compatible with stars with normal IR colors and reddening in a small range ($A_V \sim 1-2$), apart from stars with probable IR excesses. Therefore, embedded/background stars are present in a small number among X-ray sources with an IR counterpart, but are effectively absent among X-ray sources with an optical (SCB) counterpart.

Since X-ray sources identified with SCB stars will be found to have a mass larger than $0.5 M_{\odot}$ (cf. § 4.5 and Figure 11), we have plotted in Figure 5*b* the 1-Myr isochrone only down to $0.5 M_{\odot}$, and one sees that many X-ray sources now fall *redward* of it (larger $H-K$), as if they had normal colors but a lower mass, discrepant with optical photometry. If the evolutionary tracks are correct, the solution of this discrepancy might be that IR excesses are more frequent among these stars than is evident at first sight: the displacement of data points (crosses) in Figure 5*b* with respect to normal colors can in fact be accounted for simply by excess emission in the K band, as shown in the Figure. Although a very crude approximation for a real excess emission spectrum, this "excess vector" has the right slope to fit the data, while the usual reddening vector does not. Moreover, postulating large reddenings ($A_V \sim 5$) for these (many) stars would imply that they are not late-type stars (see § 4.4) but a cluster of X-ray emitting A stars, an extremely unlikely circumstance. Therefore, IR excess emission may be more widespread in our NGC 6530 stars than suggested by their apparently normal (i.e. photospheric) IR colors. Beyond these simple conclusions, the richness of 2MASS data deserves a much deeper study, that we defer to a future paper. Because of the very likely presence of IR excesses in these stars (possibly not only in the K band), we do not attempt to derive star properties (masses, ages) from an IR color-magnitude diagram, despite that the number statistics of IR-identified X-ray sources is much larger than that of optically identified ones.

4.3. Cluster Census and Morphology

We are confident that about 800 among the X-ray sources we detect in our ACIS field are confirmed cluster members (cf. § 4.1). This number is 8-10 times the number of confirmed NGC 6530 members known from previous optical studies. Since all higher-mass stars in the cluster are already known, these new X-ray objects must correspond to lower-mass stellar members (or to embedded, heavily absorbed massive stars missed by previous studies). Given that only 46 low-mass members (and candidates) were found by SCB, the increase brought about by our X-ray data in the known cluster population in this mass range is by about a factor of 15. Rauw et al. (2002) on the basis of their XMM-Newton X-ray data with its smaller source sample inferred an enlargement of only a factor of two with respect to optical studies.

With this enlarged membership, we have attempted to study the morphology of NGC 6530. The small uncertainty related to field objects will have a minimal impact on this study, since these have a uniform spatial distribution. As seen in Figures 1 and 2, clustering of X-ray sources is highest near field center. The north-east part of the FOV has a significantly lower density, while toward the south-east, a subclustering of X-ray sources can be seen. Directly counting the source density in these Figures may be misleading, however, because the point-source sensitivity decreases toward the outer parts of the FOV; some central enhancement can be expected even for a uniform source density in the sky. Therefore, we plot in Figure 6 the density of sources with ACIS count rate $\geq 3 \cdot 10^{-4}$ counts/sec, detectable across the whole FOV. This plot confirms that a strong central clustering is present, with the source density reaching a maximum at R.A.=18:04:25, Decl.=–24:22:00, which we therefore take as the NGC 6530 cluster center, and falling by a factor of 2 within a radius of $\sim 3'$ (1.5 pc) from the center. The peak density of sources with rate $\geq 3 \cdot 10^{-4}$ counts/sec is about 46.5

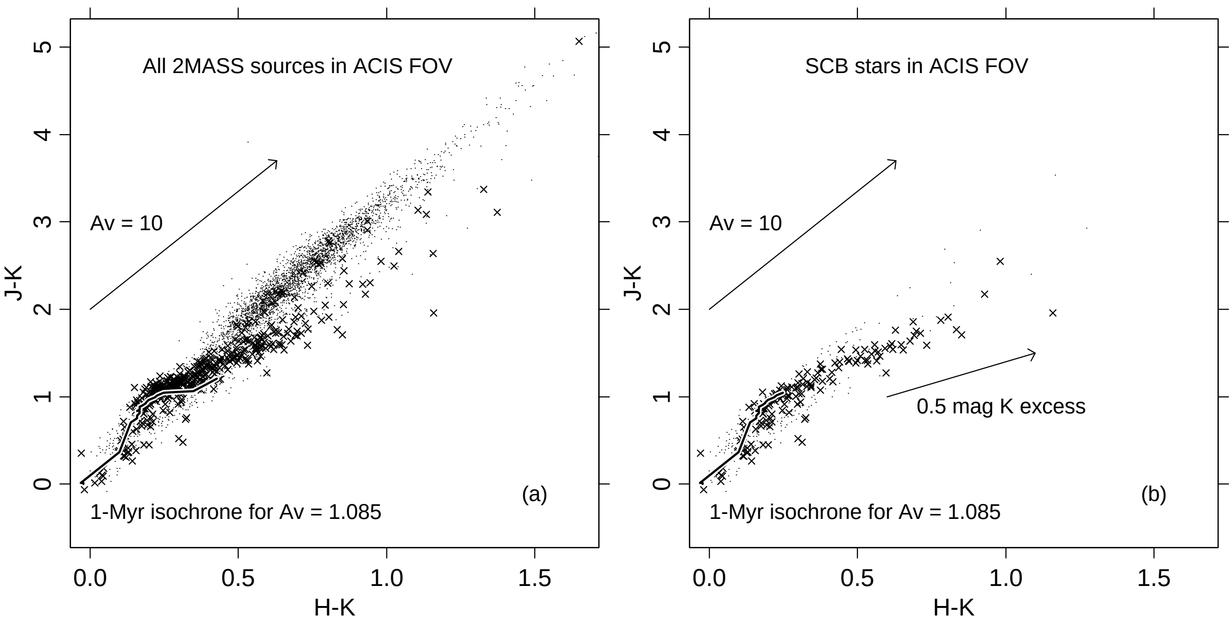

Fig. 5.— Near-IR $(H-K, J-K)$ color-color diagram of sources in the ACIS FOV. Crosses: X-ray detections, dots: X-ray undetected sources. The cluster-reddened 1 Myr isochrone, and the reddening vector are shown. (a): All 2MASS sources in FOV. (b): SCB stars only. In (b) we also show the effect of a 0.5 mag excess emission in the K band only.

stars pc^{-2} (the total peak density is 61.5 stars pc^{-2}). Figure 6 shows also that the NGC 6530 source density does not fall equally steeply in all directions. In the Figure, the arrow in the grey-level scale indicates the average source density (above the same full-FOV flux threshold) for the Galactic Plane field. In the northeast NGC 6530 quadrant the source density is the lowest, and approaches that of the Galactic Plane, while in the other three quadrants (especially in the two southern ones) it remains higher than that, until the farthest off-axis positions.

We conclude therefore that our observation has probably reached the cluster outer border in the northeast, while the cluster may extend beyond our FOV in other directions. Since the cluster center, identified as the position with the highest stellar density, appears to be near the center of our FOV, the cluster shape is asymmetrical with respect to its center. Indeed, we know that at least one young star associated with NGC 6530 namely Herschel 36, lies outside our ACIS FOV, a couple of arcmin beyond its western edge.

One would like to know just how much of the NGC 6530 cluster falls outside our ACIS FOV. Clues to this may be found in the ROSAT PSPC image, which shows that apart a few discrete sources (mainly Herschel 36 to the west and HD 165052 to the east) nearly all of the PSPC unresolved emission falls inside our ACIS field. A similar conclusion may be reached from the XMM data (Rauw et al. 2002), covering a larger field than ACIS, but pointed about 10 arcmin to the west of our field. It shows very few sources outside our ACIS FOV towards west, south and north, with the exception of Herschel 36 and its immediate neighborhood. We conclude that indeed a very large fraction of the total NGC 6530 cluster is covered by our ACIS FOV.

We have also examined why previous optical studies failed to identify this substantial NGC 6530 cluster population found in our X-ray study. Figure 7 shows spatial distributions of our X-ray sources in two different X-ray luminosity ranges, together with distributions of optical stars brighter and fainter than $V = 15$. The X-ray sources show evident clustering, while optical stars, in either magnitude range, do not (apart from the few bright OB stars, which typically do cluster). For a cluster at the distance of NGC 6530 on the galactic plane and close to the Galactic Center direction, the number of field stars is very large (even though almost no background stars are found in the SCB optical sample, as discussed in § 4.2) and precluded a statistical determination of the cluster population of late spectral types, as noted by previous studies such as Thé (1960).

We have computed the expected number of foreground field stars brighter than V=17 falling in the ACIS FOV towards NGC 6530 (using data from Allen 1973 which, for a cluster distance of 1800 pc and average extinction $A_V \sim 1$, turns out to be of 720 stars, even larger than the number of X-ray undetected SCB stars in the FOV (391 stars, see § 3.3). For a smaller cluster distance of 1300 pc (Walker 1957) the expected number becomes 356 stars, very close to the observed number. In any case, we do not expect many background stars to be contained in the SCB sample.

Compared to SCB field stars, an even larger density of field stars (both foreground and background) is found in the 2MASS data, as already seen in § 4.2. This emphasizes how crucial sensitive, high-resolution X-ray data are for a proper study of such very young star clusters.

4.4. H-R Diagram

To understand better the nature of the stellar population selected through our X-ray data, we have located their optical counterparts on a $(V,\ V-I)$ H-R diagram of the NGC 6530 region, using SCB optical data, as shown in Figure 8. A few stars fainter than $V = 17$ are PMS cluster members selected by SCB from their Hα excess.

This diagram proves to be very rich in information. Examining Figure 8, we note: (1) an upper main sequence (as reddened by SCB and indicated with vector at upper right); (2) a swarm of stars whose lower envelope shapes the main sequence at the NGC 6530 distance, mostly undetected in X-rays, labeled "field-star main sequence" in the Figure; (3) another swarm of X-ray detected stars, distinctly to the right of "main sequence" field stars, and mostly at faint V magnitudes; and (4) with still redder $V - I$ color, a much less numerous population of stars, presumably foreground.

Since we have already established that most stars detected in X-rays are cluster members, the position occupied by the bulk of X-ray detections defines the NGC 6530 cluster locus in the H-R diagram. Accordingly, we have drawn a trapezoidal region enclosing them in Figure 8, with (reddened) colors corresponding to G-K-M stars, and we have labeled it "cluster locus". The number of X-ray detected G-K stars in the "main sequence" and "foreground" regions is of about 12-15, compatible with the estimated number of contaminating field objects among optically identified sources. Therefore, we regard all X-ray detections in the "cluster locus" as genuine NGC 6530 members, with no more than a few spurious objects among them. On the other hand, the probability that X-ray detected stars outside the cluster locus belong to the cluster is expected to be very small. In most X-ray studies of star-forming regions with a well-defined member list, e.g., as in the Orion Nebula, X-ray detected and undetected stars are found to be well mixed in the H-R diagram (see e.g., Feigelson et al. 2002, Flaccomio et al. 2003). We therefore assume that there will be hardly any NGC 6530 members among the X-ray undetected stars that fall outside our cluster locus.

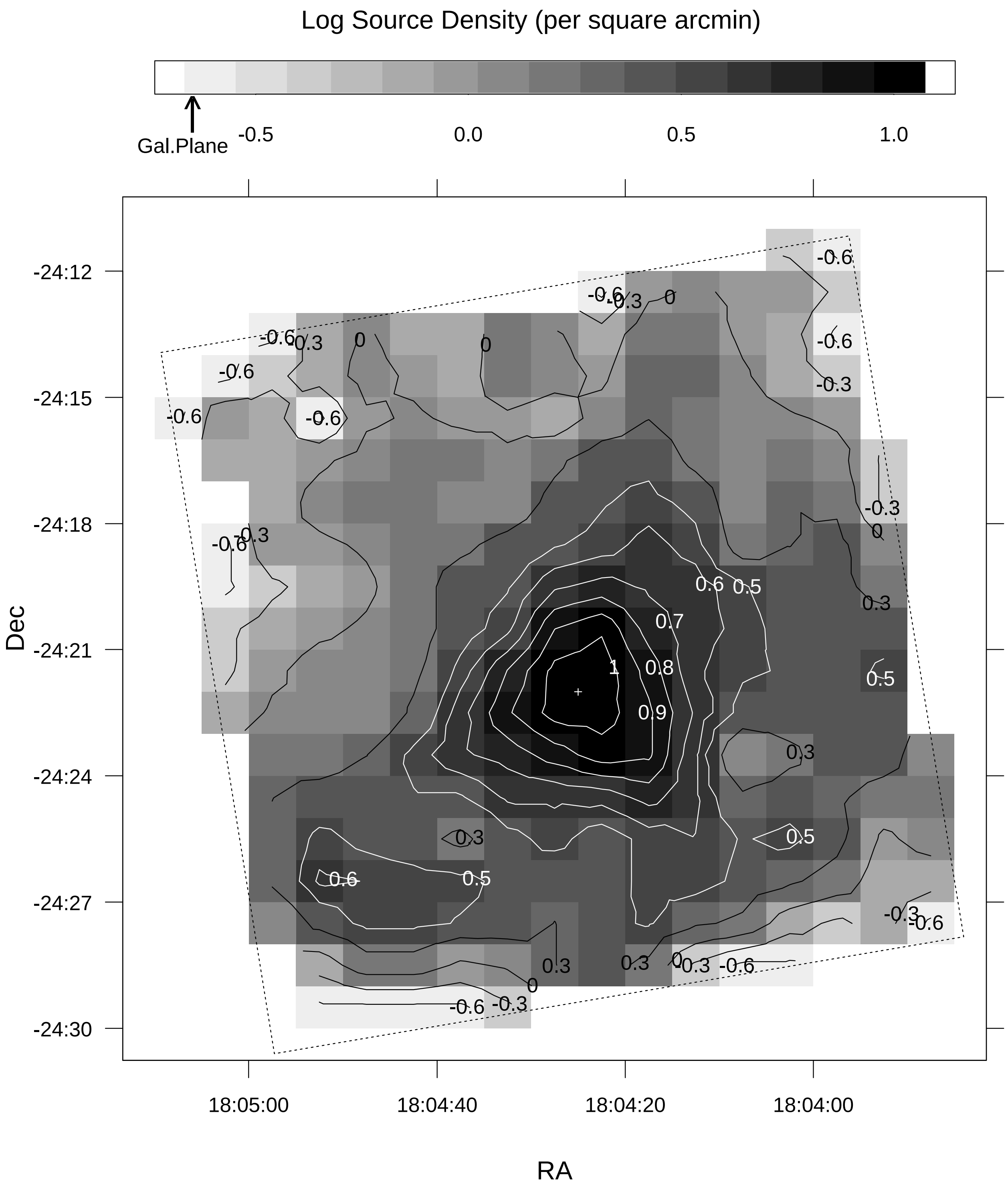

Fig. 6.— Grey-level map of detected source density in NGC 6530 (only sources with ACIS count rate $\geq 3 \cdot 10^{-4}$ counts/sec, detectable across the whole ACIS field), with contour levels. The assumed cluster center is indicated by a small cross. The arrow in the upper grey-level scale indicates the average source density in the reference Galactic Plane field.

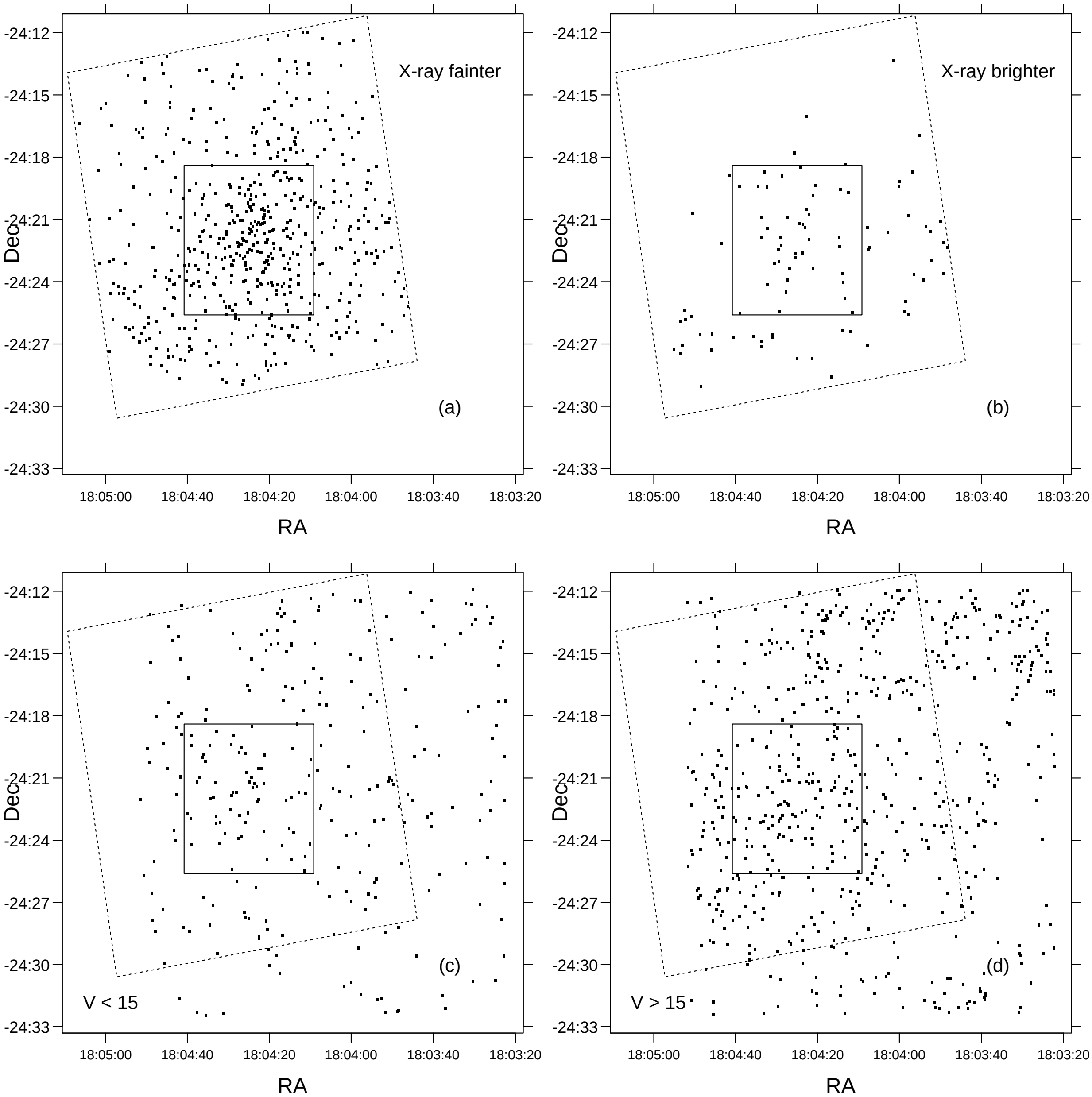

Fig. 7.— Spatial distributions of (a): X-ray sources with ACIS count rate in the range $3 \cdot 10^{-4} - 3 \cdot 10^{-3}$ counts/sec; (b): X-ray sources with ACIS count rate $\geq 3 \cdot 10^{-3}$ counts/sec; (c): all stars with $V < 15$; (d): all stars with $V \geq 15$. Note that, apart from visually bright stars evident in Figure 1, there is no obvious clustering of optical stars in any magnitude range, as found in previous studies. The dotted lines indicate the ACIS FOV, while the solid lines indicate a reference square region of side 7.2 arcmin, centered on cluster center as defined in Figure 6.

For field stars at distances just a little closer than NGC 6530, the main sequence is very well defined (cf. § 1) as the lower envelope of dots in Figure 8, with only two stars below it, confirming the absence of background field objects, with the two exceptions probably seen through small holes in the molecular cloud (or perhaps representing foreground white dwarfs). The reddening of background stars must therefore be so large that they would appear at much fainter magnitudes than the SCB catalog limit. The direction of the reddening vector direction, as shown in the Figure, is such that stars in the cluster region cannot be more distant, highly reddened stars.

Most X-ray detected stars have $V-I$ colors of K stars. None has M star colors, probably since M stars in the cluster are fainter than the SCB magnitude limit, and all M stars in SCB are low-mass foreground stars. Among stars bluer than G type, we consider all O and B stars in the FOV to be cluster members because of their rarity in the field, as found in previous studies. Stars of intermediate type (A and F) are seen in the H-R diagram of Figure 8 to be mostly X-ray detected if they are brighter than $V = 13$; because of their large number these X-ray sources must also be cluster members. Therefore, we consider all stars earlier than type G and with $V < 13$ to be highly probable cluster members. The percentage of X-ray detected stars in the range B3-F5 is 49% (25/51) for $V < 13$; including fainter (mostly field) F stars halves this percentage.

In order to compare our NGC 6530 member selection with that of previous optical studies, we show in Figure 9 a $(V,\ B-V)$ diagram for NGC 6530, plotting X-ray detected and undetected stars, together with stars found by van Altena and Jones (1972) to have a proper-motion membership probability > 50%. In addition, we indicate with horizontal lines approximate magnitude limits for various previous studies (cf. § 1). A number of early type stars have low proper-motion membership probability, suggesting that this indicator has limited value. Nevertheless, we find that many stars of types B and A, and $V \leq 13$ are both proper-motion members and X-ray detected, strengthening our assertion that these stars are indeed cluster members. The usefulness of the proper motion study of van Altena and Jones (1972) is confined to these brighter stars because of the study's magnitude limit at around $V = 13.6$. The inability of Thé (1960) and SCB to detect the lower-mass cluster locus can be understood in view of both the large number of field stars and the fact that in such a young cluster low-mass stars are still in their PMS stages. They are regularly found in a wide band above the main sequence in the H-R diagram, not in a narrow and well defined ZAMS locus. This "dilutes" their appearance on the H-R diagram and makes them unrecognizable against the large number of foreground field stars.

To test the validity of our "cluster locus" selection in the $(V,\ V-I)$ diagram, we plot in Figure 10 the spatial distributions of stars in this locus (a), and stars in the "main sequence" locus (b). It is obvious that while "cluster locus" stars are indeed clustered around the NGC 6530 center, and are much less numerous outside our ACIS FOV, to the south and to the west, "main sequence" field stars are much more evenly distributed across the whole region, with absolutely no clustering towards cluster center. This strengthens our contention that most stars in the "cluster locus" are indeed cluster members. This locus contains 158 X-ray detected and 88 X-ray undetected stars. While the cluster membership is virtually assured for all detections, membership for non-detections is much more uncertain. If the NGC 6530 cluster ends exactly at the edge of our FOV (a reasonable approximation, as discussed above), we can estimate the number of non-members in the cluster locus inside our FOV from the space density of cluster-locus objects outside the FOV. A density 0.41 ± 0.05 cluster-locus stars per square arcmin, times the ACIS FOV area common to SCB, yields 104 ± 12 field stars in the cluster locus within our ACIS FOV. This number (within uncertainties) is the same as the number of undetected stars in the cluster locus, indicating that most are non-members. Since we do not know exactly where the NGC 6530 cluster border lies in the sky, however, this is an overestimate of contamination in the cluster locus, and we will admit in the following also the possibility that a fraction of the X-ray undetected stars in this locus may be NGC 6530 members.

In the following we therefore regard as confirmed cluster members: (1) all O and B stars; (2) all A and F stars brighter than $V = 13$; (3) all X-ray detected stars falling in the "cluster locus" of Figure 8; (4) all Hα emission PMS stars selected by SCB (including PMS candidates), 39 of which fall in our ACIS FOV, regardless of their X-ray detection. These stars will be collectively indicated as "cluster stars". X-ray undetected stars falling in the H-R diagram "cluster locus" are of uncertain status and will be indicated as "possible members."

4.5. Masses and Ages

Figure 11 provides a comparison of the H-R diagram positions of stars in our ACIS FOV with the predictions of theoretical PMS evolutionary tracks[3] (Siess, Dufour and Forestini 2000; SDF), reddened using the average NGC 6530 values found by SCB. Here we have omitted all optically bright stars, already on the main sequence, and very red ($V - I > 3$) stars foreground field stars. Using the SDF models, we have derived from the diagram

[3]These models have proven to be consistent with dynamical stellar masses (Simon, Dutrey and Guilloteau 2000) and have already been used in the interpretation of *Chandra* X-ray data on the Orion Nebula Cluster by Flaccomio et al. (2003).

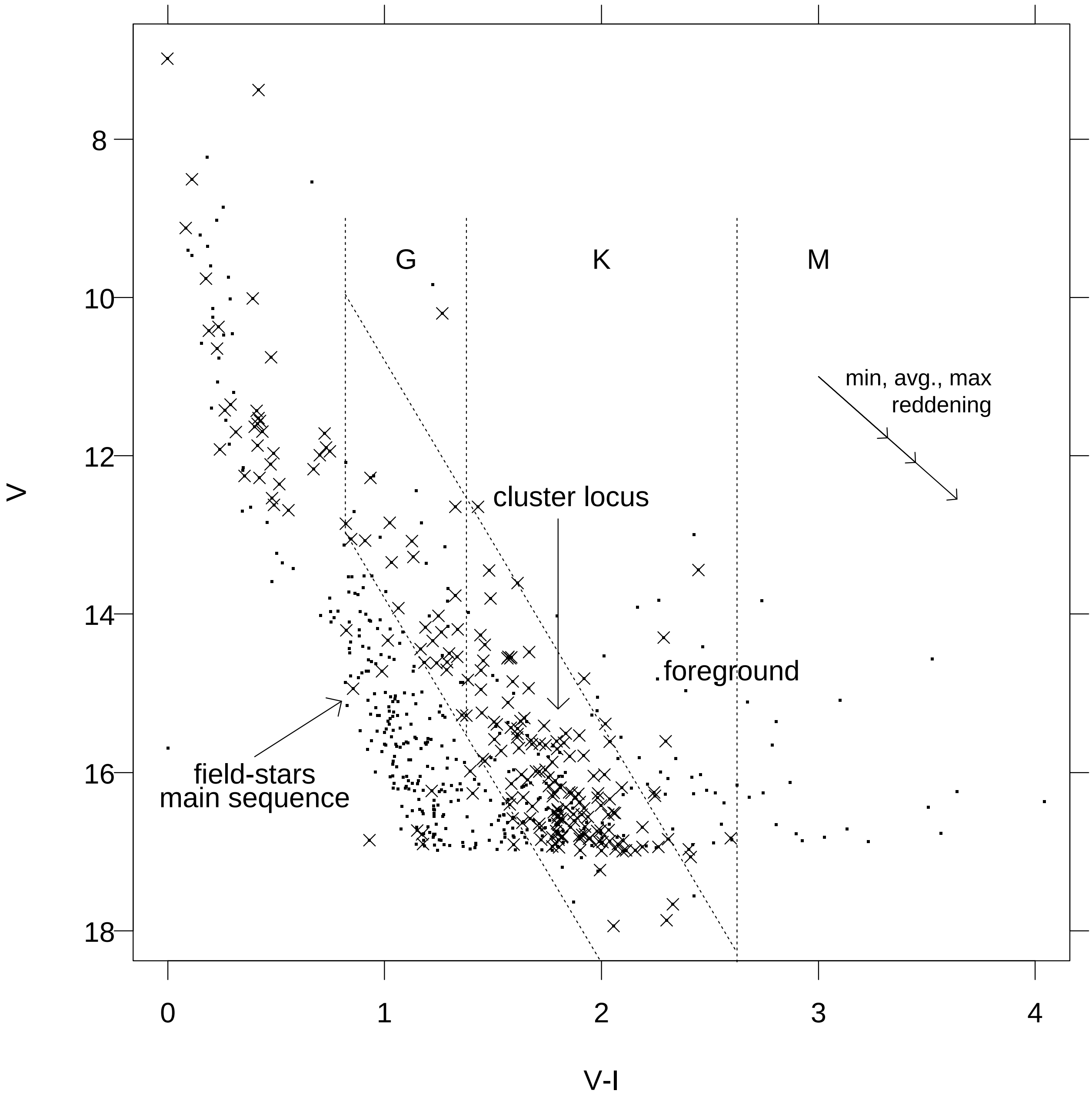

Fig. 8.— Color-magnitude (V, $V - I$) diagram for NGC 6530 (from SCB data). The average reddening correction and its range are indicated. X's: X-ray detected stars; dots: X-ray non-detections. A region is indicated where most X-ray detected stars with G-K (de-reddened) $V - I$ color are found, that we call "cluster locus". Blue-ward of it, we identify a field-star "main sequence" (envelope of field-star main sequences up to the cluster distance). Note that there is an apparent lack of stars more distant than NGC 6530, probably because they are completely obscured by the dark cloud just behind the visible cluster. See text.

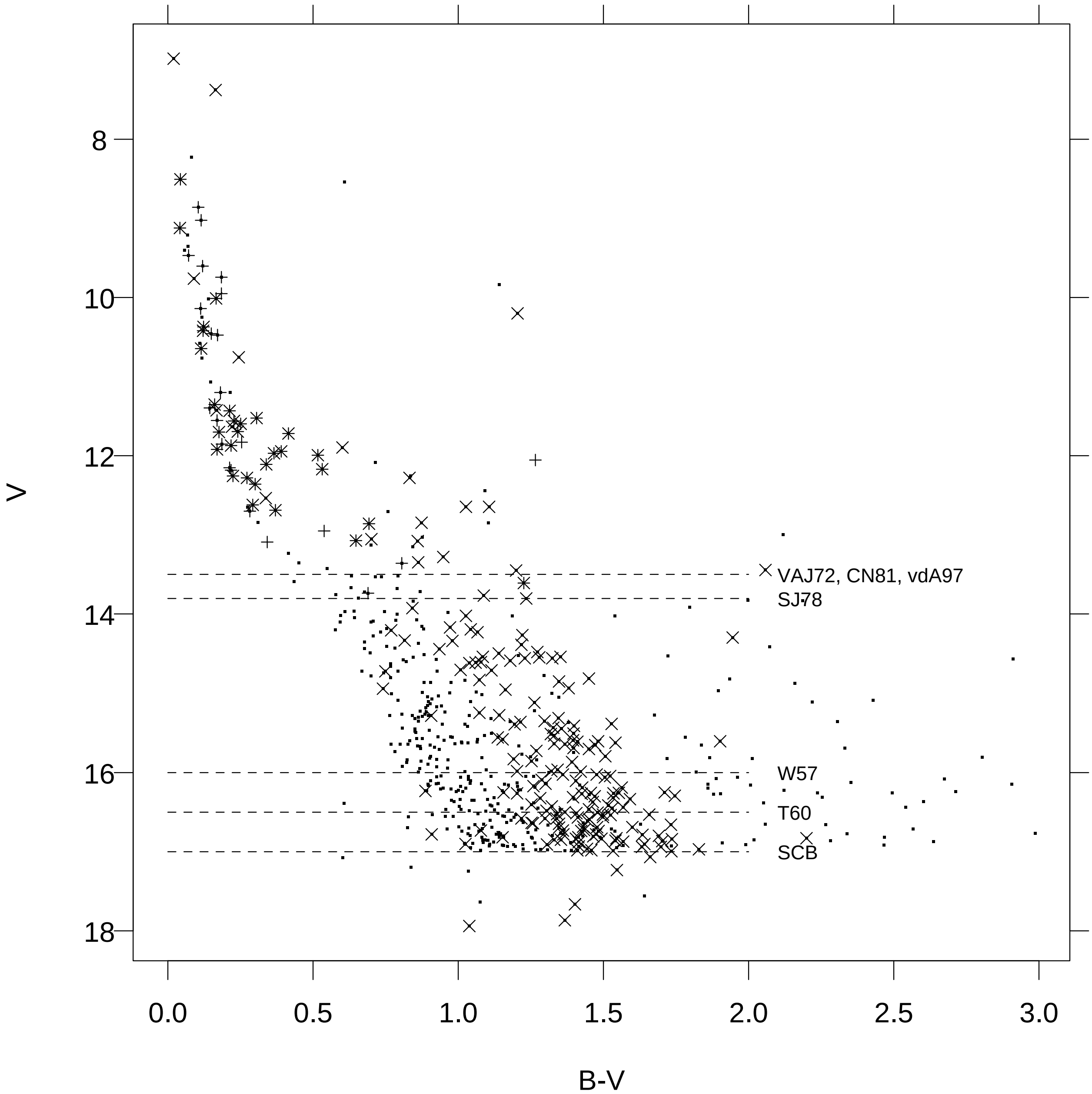

Fig. 9.— Color-magnitude (V, $B - V$) diagram for NGC 6530. X's: X-ray detected stars; dots: X-ray non-detections; plus signs: stars with proper-motion membership probability $> 50\%$ according to Van Altena and Jones (1972) (X-ray detected, proper-motion members show up as asterisks). Dashed horizontal lines indicate magnitude limits from different optical studies of NGC 6530: Van Altena and Jones (1972, VAJ72), Chini and Neckel (1981, CN81), van den Ancker et al. (1997, vdA97), Sagar and Joshi (1978, SJ78), Walker (1957, W57), The (1960, T60), and SCB.

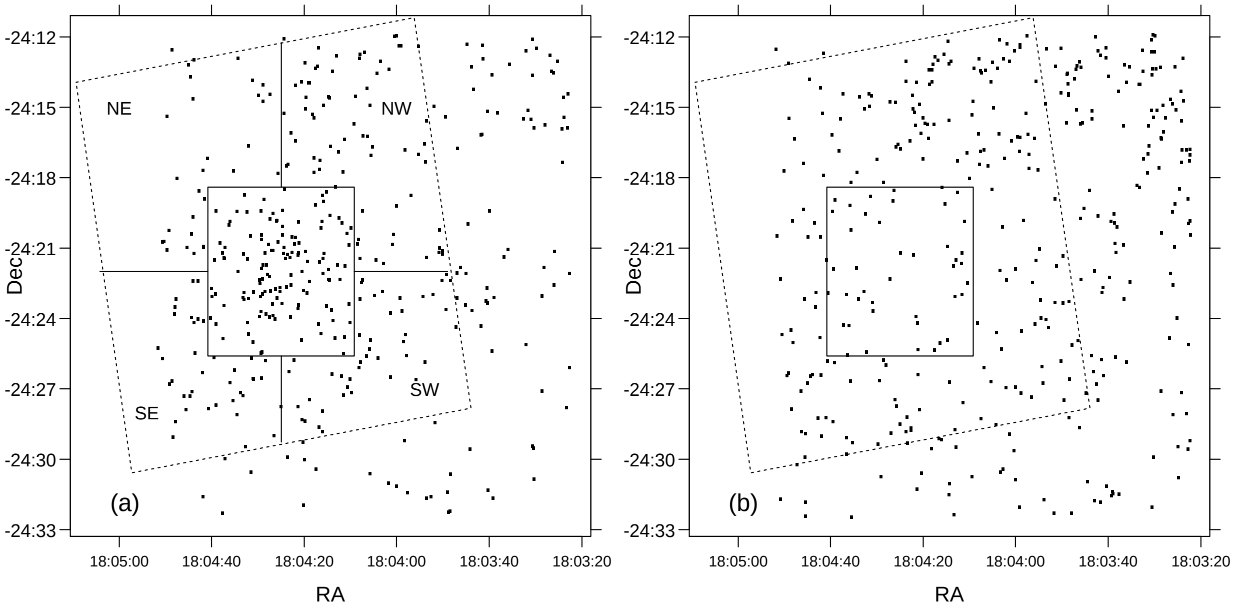

Fig. 10.— Spatial distribution of (*a*) "cluster-locus" stars, and (*b*) "main-sequence" (putative field) stars, including also stars outside the ACIS field of view. The difference between these distributions is obvious and strengthens our assumptions on the nature of the two subsamples. Also identified in (*a*) are different subregions discussed in the text.

shown in Figure 11 masses and ages for our cluster stars not yet on the main sequence. The plotted ZAMS in Figure 11 is reddened with the average cluster extinction, while a differently reddened ZAMS is appropriate for field stars.

In the Figure we have also indicated with triangles optical irregularly variable stars in our ACIS FOV (29 stars), from the General Catalogue of Variable Stars (Kholopov et al. 1998). These stars are typically found in star-formation regions, among low-mass PMS stars (e.g., T Tauri stars). They share the same locus in the H-R diagram as the X-ray detected cluster population and are thus stars in the same mass range and evolutionary stages. Ten of these variable stars are also strong Hα emitters, and all but 4 are detected in X-rays. Only two of these latter four are plausible cluster members from their position in the H-R diagram, one also selected from Hα. Hence including variable stars adds little to the NGC 6530 population already selected.

In Figure 8 we have shown the average reddening found by SCB in NGC 6530, as well as its minimum and maximum value. These values were derived from the $(U-B, B-V)$ color-color diagram of OB stars. In Paper II we present indications on the basis of our ACIS X-ray spectra that the average absorption of lower-mass stars may be higher, on average by a factor of two (provided that the thermal structure of these stars' coronae is satisfactorily reproduced by our models, and that a constant gas to dust ratio is present towards all cluster stars). An examination of the $(U-B,\ B-V)$ diagram for all cluster stars (i.e., confirmed members) shows that lower-mass stars have a larger scatter than massive stars, indicating a larger range of differential extinction, with higher average values. From Figure 11 we see that differential reddening may displace stars in the H-R diagram along a direction almost parallel to isochrones in the part of the diagram where most cluster stars are found. Therefore, age estimates are little affected by extinction uncertainties (within twice the range found by SCB), while mass estimates are much more affected (for example a star with $M = 1M_{\odot}$ may be mistaken with a more reddened star with $M = 1.5M_{\odot}$). Masses for possibly embedded objects are instead much more uncertain.

Figure 12a shows the age distributions of NGC 6530 members found in different non-overlapping subregions, namely a central region plus four outer regions. Despite a large scatter, there is a systematic difference between these regions: stars in the northwestern outer region appear to be definitely older than stars in the cluster center. To a lesser extent this is true also of stars in the northeast. On the contrary, stars in the southeast are on average younger than cluster center, with a smaller spread, while stars in the southwest seem to have a mixture of ages, some similar to cluster center, and some much younger. This southwest subregion apparently contains a heterogeneous stellar population, with an age spread larger than elsewhere in the cluster. It is also closest to the Hourglass region, which contains the very young star Herschel 36.

On the basis of the 'displacement' between the NGC 6530 stellar cluster and the more embedded, probably protostellar object Herschel 36 and the Hourglass Nebula, it was proposed that star formation in this region occurred in a sequence, starting near the NGC 6530 center and proceeding towards west. In this scenario, one would expect to find younger stars in the western part of our FOV, lying very close to the Hourglass. Our data suggest instead a different scenario, where star formation has progressed from north to south, not from east to west. Stars in the northwest were the initial generation of stars, now fully emerged out of the molecular cloud (stars in this region are found in Paper II to have the smallest X-ray absorption), then the bulk of the cluster formed (in the central region), and later stars formed more to the south and southwest (including the Hourglass region). This can be seen more clearly from Figure 13, which plots the spatial distributions of cluster stars in three different age ranges: age less than $5 \cdot 10^5$ yrs (filled circles), age between $5 \cdot 10^5$ and $2 \cdot 10^6$ yrs (plus signs), and age greater than $2 \cdot 10^6$ yrs (empty circles). It is obvious that very young stars are dominant in the south/southwest, comprise a smaller fraction in the center, and are totally absent in the northwest.

It is also interesting to note that the very young stars found in the south share the same spatial distribution as the X-ray flaring sources (cf. § 4.7). Moreover, the X-ray bright stars in the southeast follow rather closely the shape of an Hα bright rim, which is evident at the bottom left of Figure 1 and appears to be the edge of a denser portion of the molecular cloud, excited by the radiation of the nearby O stars (primarily 9 Sgr) and probably also compressed by the winds of the massive star(s). In the same region, Tothill et al. (2002) have found a series of molecular cloud cores, probably undergoing collapse. The association of a very young PMS group and a perturbed, compressed cloud is not likely to be accidental; it is probably instead an example of genuine induced star formation, caused by the action of nearby massive stars.

The median age of cluster stars in the central region is $8 \cdot 10^5$ yrs, slightly younger than the 1.5 Myr derived by SCB for the massive NGC 6530 stars, and compatible with the possible ages they find for low-mass PMS stars. Since there may be uncertainties in the evolutionary models, especially when comparing high- and low-mass stars, we regard high- and low-mass stars in the same NGC 6530 subregion as essentially coeval. This age similarity between massive and low-mass stars is unlike that found in another very young cluster, NGC 6231, where Sung, Bessell and Lee (1998) find that the low-mass stars are much older than massive stars. The age spread we observe for the whole NGC 6530 cluster is similar to that (4 Myr) found by SCB, while the age spread we find in each subregion is smaller.

Because X-rays with energies above 1 keV can emerge from deep within a molecular cloud, our sample probably contains stars much more reddened than found by SCB. However, a difference in reddening between stars in the northwest and those in the south is unlikely to be the only reason why these stars appear to have different ages. Since age is relatively insensitive to reddening in this part of the H-R diagram, a large reddening for the southern stars should be invoked to make all stars have the same age. If this were the case, stars in the south would be fainter and harder to detect, both in the optical and X-rays. But in this region there is no deficit of optical stellar counterparts; instead there is an excess of (bright) X-ray sources with respect to northern regions. Moreover, a difference only in reddening would not explain the spatial coincidence of these apparently younger stars with flaring X-ray sources. Nor are the flaring sources more absorbed than other X-ray sources: as noted in § 4.7 and § 4.8, flaring sources and strongly absorbed X-ray sources have very different spatial distributions, with the latter uniformly spread over the FOV, not concentrated towards the south.

We have also studied the distribution of stellar masses in the same subregions, as shown in Figure 12*b*. An apparent correspondence between the age and mass distributions, i.e., with older (younger) regions containing also more (less) massive stars and vice versa, is very likely due to a selection effect of the combination of the evolutionary path of low-mass stars in the H-R diagram with the V magnitude limit of the SCB catalog. If the stars in a region are younger, they are still high on their Hayashi tracks, and therefore stars of lower masses are above our magnitude limit. On the other hand, in an older region only more massive stars are above the same limit. Therefore, with the current magnitude limit it is difficult to discriminate between an age and a mass effect (but at least one of the two is really present). Moreover, mass determinations from evolutionary tracks are more sensitive to reddening uncertainties than age determinations. The magnitude limit of the SCB catalog ensures that we have a complete sample of stars with masses above $1.5M_{\odot}$, while the coverage of lower-mass stars is increasingly less complete, with the lowest selected cluster members having a mass of $0.5M_{\odot}$ (Figure 11).

A mass segregation effect with the (apparent) observed pattern, however, namely a south-to-north mass gradient whereas the bulk of the cluster lies in the middle, seems highly unlikely, and we therefore strongly favor the interpretation as an age evolution rather than a mass difference. To settle this question definitively, a deeper photometric catalog is needed, and one will be available in the near future (L. Prisinzano et al., in preparation).

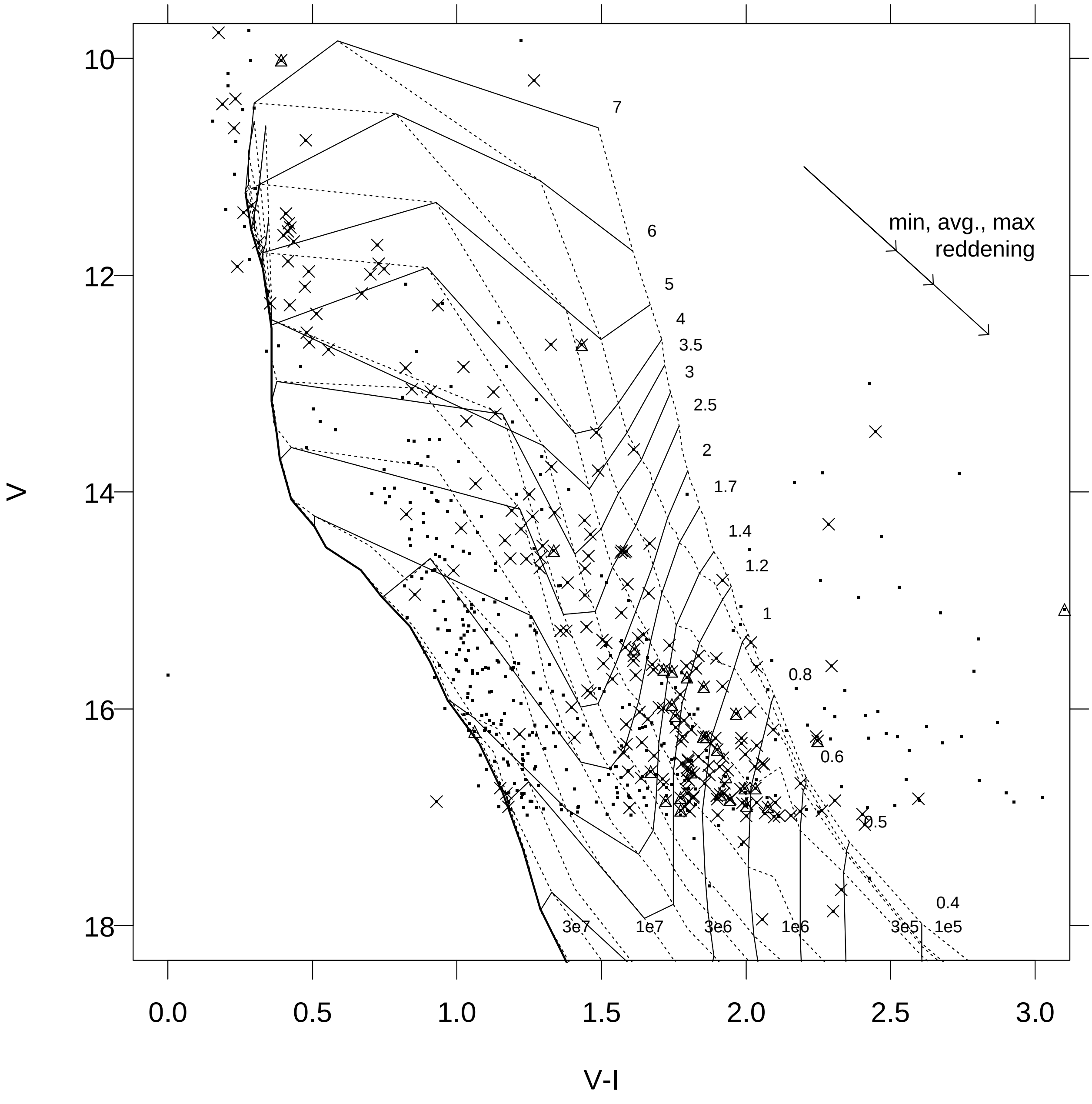

Fig. 11.— Color-magnitude ($V,\ V-I$) diagram of all stars in the ACIS FOV with $V > 10$, with overlaid (reddened) evolutionary tracks (solid) and isochrones (dotted) from Siess et al. (2000). Symbols are as in Figure 8, with the addition of triangles to indicate optical variable stars. Note that the plotted ZAMS is reddened with the average cluster extinction, while a differently reddened ZAMS is appropriate to field stars.

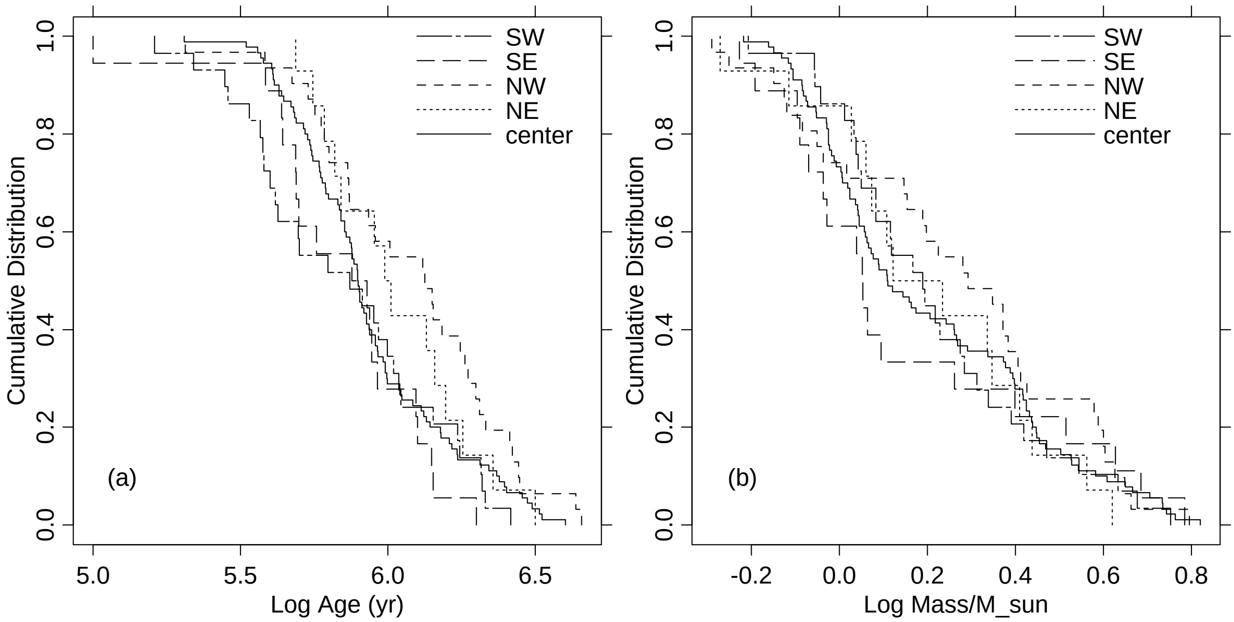

Fig. 12.— Age and mass distributions for X-ray detected stars in "cluster locus" belonging to different spatial regions, identified in Figure 10. (*a*): age distribution; there is a clear age difference between the selected samples in different regions, especially between the N-W and S-E regions. (*b*): mass distribution; a difference is visible, but this may be due to the combined effect of an age difference and the optical photometry V limit.

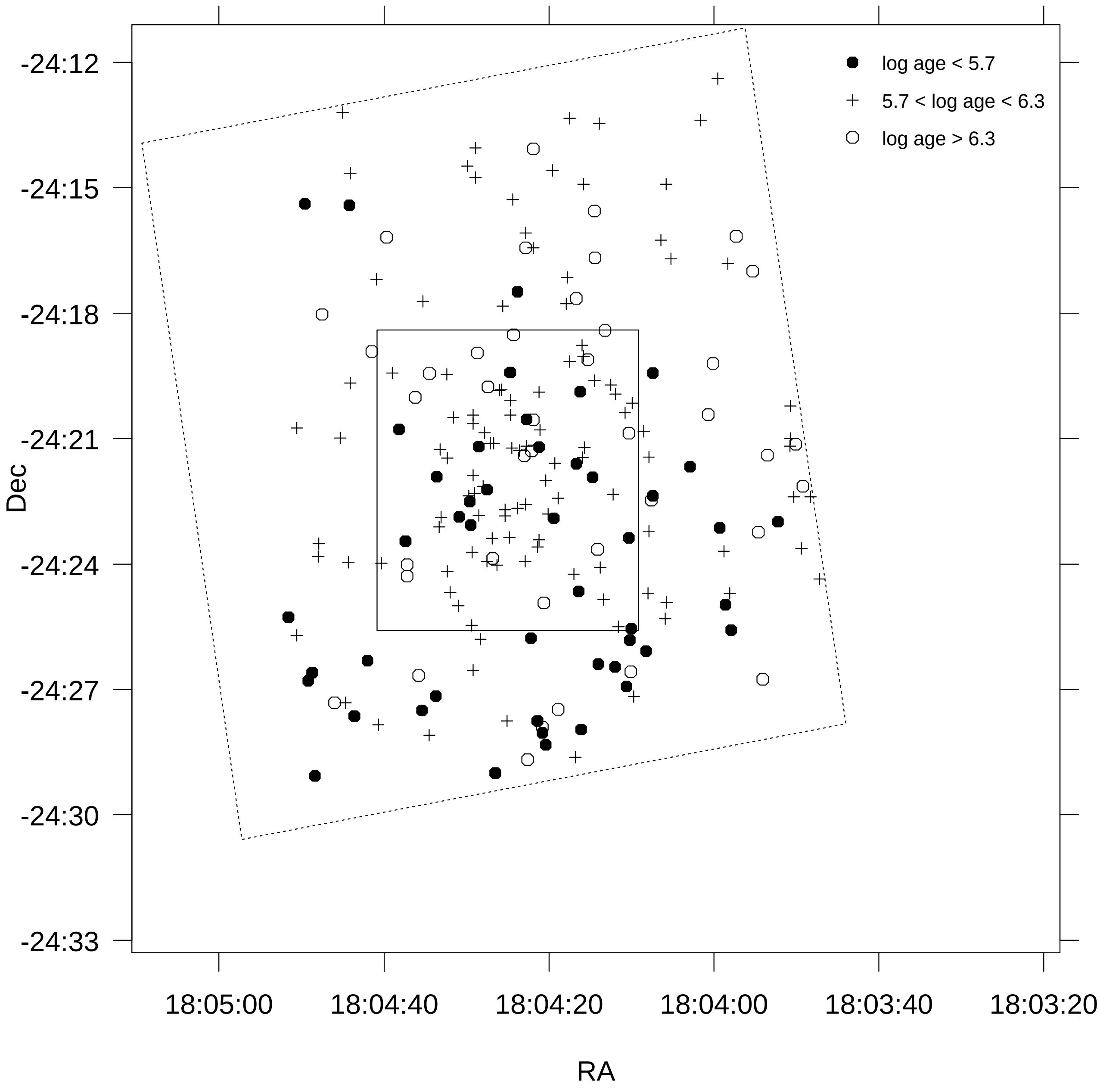

Fig. 13.— Spatial distribution of X-ray detected stars in three different age ranges. Filled symbols: log age $<$ 5.7 Myr; pluses: log age between 5.7 and 6.3 Myr; empty symbols: log age $>$ 6.3 Myr. Note the prevalence of very young stars in the southern part.

4.6. Stars with Hα Emission

We have compared the cluster population selected in X-rays with that selected using Hα by SCB in Figure 14, a (V, $R - H\alpha$) diagram, where $R - H\alpha$ is the Hα emission index reported by SCB. Stars with strong Hα emission are found in the right part of this diagram. Triangles indicate optical variables, some of which are also stars with strong Hα, while plus signs represent stars exhibiting X-ray flares, two of which are also strong Hα stars.

First, we note that 10 stars with strong Hα are not detected in X-rays, a sizable fraction of the total number of strong Hα stars. These stars are confirmed cluster members both because of their Hα emission and of their position in the H-R diagram. On the other hand, most X-ray detected stars (confirmed members as well) have an Hα emission not distinctly different from X-ray undetected stars (mostly non-members). Therefore, X-ray and Hα observations provide two complementary means of selecting low-mass PMS stars in a star-forming region such as NGC 6530, with stars escaping one method being easily found by the other. It should be pointed out however, that, within the magnitude limit of the SCB catalog, X-ray imaging appears to be much more efficient in selecting these PMS stars.

In the Figure, solid and dotted segments indicate median $R - H\alpha$ values for X-ray detected and undetected stars, respectively, in different V magnitude intervals. Although no clear-cut separation is present, X-ray detected stars have systematically larger $R - H\alpha$ indices than undetected stars. The median $R - H\alpha$ values (not shown) for X-ray undetected cluster-locus stars are close to the rest of undetected stars in all magnitude ranges, suggesting again that most of these stars are not cluster members, as already found in § 4.4. The behavior found for X-ray detected stars indicates that most cluster stars, although not showing a very strong Hα emission, have some Hα emission in excess of the main-sequence star level. This might be due to enhanced chromospheric activity, which parallels enhanced X-ray activity in stars of very young ages, or to residual circumstellar phenomena, where the star interacts with a surrounding accretion disk, as is thought to happen in strong-Hα stars. This latter option is maybe favored, since at the very young age found for NGC 6530 stars most stars in other star-forming regions (e.g., Orion) are found to have still an accretion disk and to interact with it to some extent. While a more precise classification of these stars must wait for high-resolution optical spectra of these stars, some clues may come from the analysis of the just released IR data from the 2MASS survey. This is however beyond the scope of this paper. A detailed analysis of the respective X-ray emission levels of weak- and strong Hα stars, and of the connection between PMS accretion and X-rays, will be presented in Paper II.

Since another indicator of circumstellar accretion in PMS stars is UV excess, we have also studied where our cluster-locus stars fall in a (V, $U - B$) diagram, shown in Figure 15 (field stars are not plotted). In this plot, we have also indicated Hα emission stars with circles. At least a dozen stars in the cluster locus have strong violet excesses, suggesting active pre-main-sequence accretion. Most of them have $V \geq 16$, and $V - I$ colors of K stars. Nearly all of the UV excess stars are already selected as members either through Hα (mostly) or X-rays (a smaller number), and therefore an UV selection would not add much to our knowledge of the cluster. Eight UV excess stars are also optical variables.

4.7. X-Ray Variables

Some of our X-ray sources show flare-like X-ray variability (cf. § 4.6). While this will be studied in detail in a further paper (F. Damiani et al., in preparation, hereafter Paper III), we discuss here some implications for the study of the cluster population. Various types of X-ray variability are found in NGC 6530, but here we focus only on sources showing 'classical' X-ray flares.

Figure 16 shows the spatial distribution of flaring X-ray sources (filled circles). The spatial nonuniformity is obvious, and with good source statistics. This distribution, heavily concentrated towards south-southwest, is very similar to the distributions both of the youngest cluster stars (Figure 13), and of the brightest X-ray sources (Figure 7*b*), while it is unlike the distribution of the bulk of X-ray detected sources (Figure 7*a*). We therefore conclude that in NGC 6530 frequent and intense X-ray flares are preferentially associated with the youngest of PMS stars and decline rapidly afterwards, even at ages of only 2 Myr (typically found in the northwest region, where only few flaring stars are found).

By comparison, stars with strong Hα emission in NGC 6530 are characterized by a much broader spatial distribution, across practically the entire cluster (Figure 16, circles). In other star-formation regions, Hα emission is found in PMS stars with a large range of ages, thus not only in the earliest phases of evolution. In the H-R diagram, it is often found that strong Hα stars share their locus with weak Hα stars, so that the time scales for decrease of circumstellar activity vary from star to star, over a wide range. This indicates that strong X-ray flaring is a more typical feature of the very youngest PMS stars than strong Hα emission is.

4.8. Hard X-Ray Sources

We now study the subset of detected X-ray sources with hard X-ray spectra, defined as having at least 3/4 of total counts with energy above 1.5 keV. At these X-ray energies,

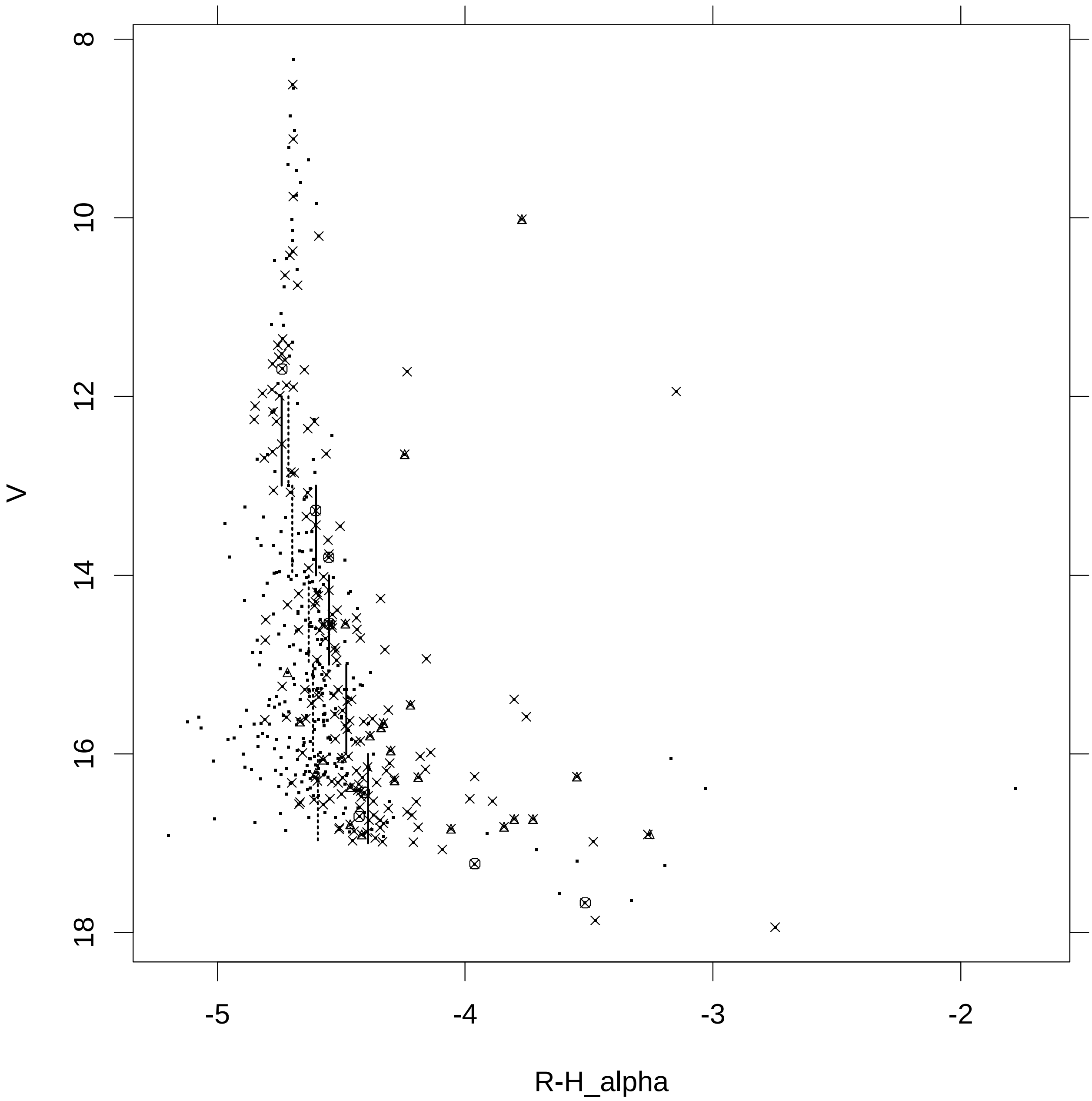

Fig. 14.— Diagram $(V, R - H\alpha)$ for the whole NGC 6530 ACIS field. X's are X-ray detected stars; dots are X-ray non-detections, open circles denote stars exhibiting X-ray flares; triangles show optically variable stars. Stars with Hα excess appear in the right part of this diagram and not all are X-ray detected. Solid and dotted vertical segments indicate median $R - H\alpha$ values for X-ray detected and undetected stars, respectively, in different V magnitude intervals.

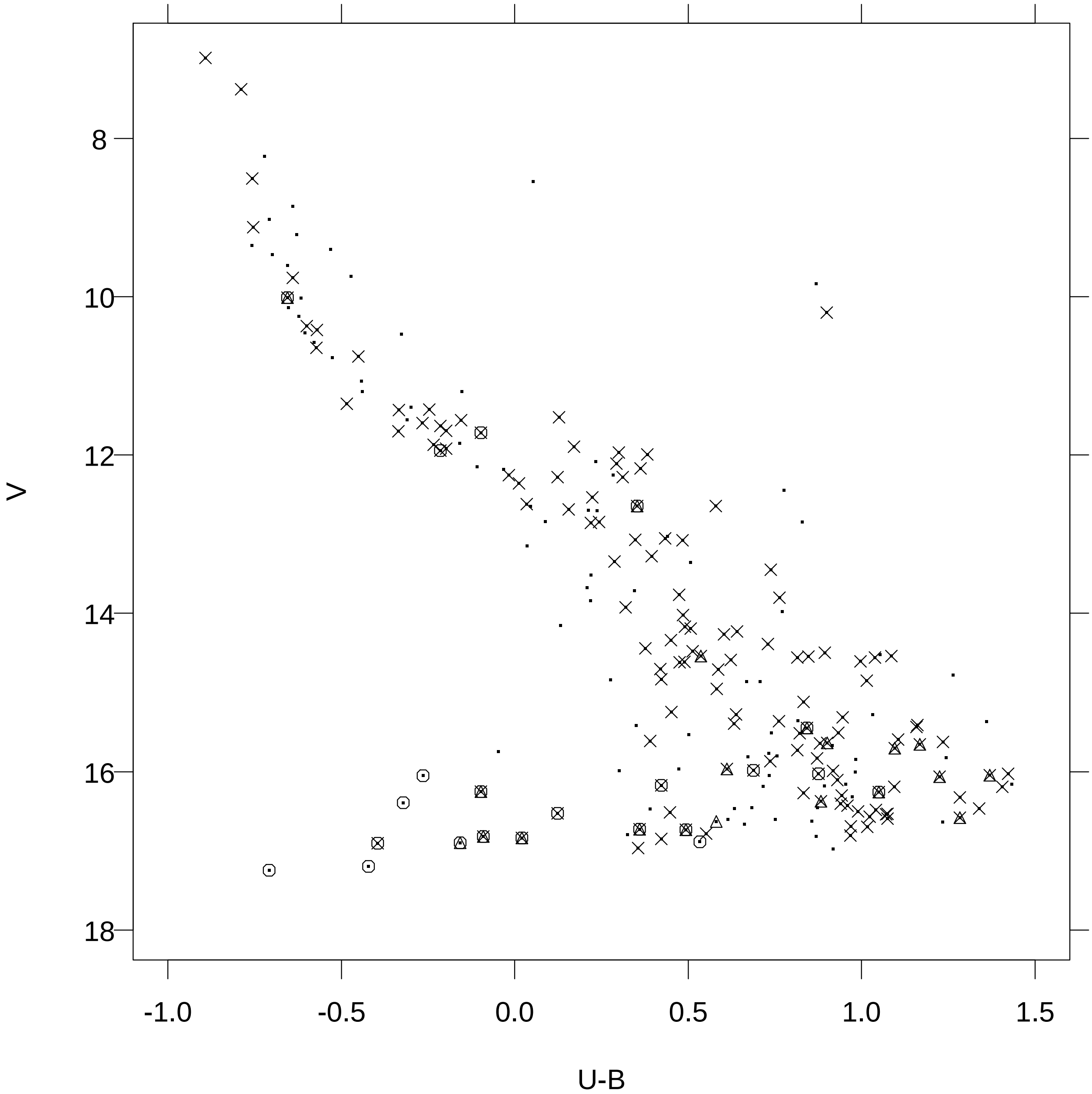

Fig. 15.— Color-magnitude ($V,\ U-B$) diagram for NGC 6530. For $V > 13$, only stars in the "cluster locus" are plotted. X's: X-ray detected stars; dots: X-ray non-detections; circles: Hα-excess stars; triangles: optical variable stars. Stars with $V > 16$ and $U - B < 0.25$ have strong violet excesses.

absorption is much smaller compared to lower energies, providing an opportunity to peer deeper into the cloud, or even to detect background objects, unrelated to the cluster.

In our ACIS FOV we find 101 such hard sources, of which only 7 have an optical counterpart in the SCB catalog, a much smaller fraction than the overall fraction of optically identified X-ray sources (24.9%). The counterparts of most hard sources are therefore either very faint and/or heavily obscured objects. The number of hard sources is compatible with the hypothesis that all of them are background objects (cf. § 4.1). However, the ACIS count rate distribution of such sources has a median of $4.3 \cdot 10^{-4}$ cts/sec, intermediate between the median count rate of the whole NGC 6530 field ($5.9 \cdot 10^{-4}$ cts/sec) and that of the reference Galactic Plane field of § 4.1 ($2.9 \cdot 10^{-4}$ cts/sec). In the Galactic Plane field, absorption of distant objects is not as large as in our NGC 6530 field. If it were the same, the hard sources would be detected with higher count rates, becoming thus even less compatible with the Galactic Plane values. Therefore, this hard-source subsample is unlikely to be composed predominantly of background objects, but rather should be largely composed of embedded cluster members.

To verify this, we have plotted in Figure 16 the spatial distribution of such hard X-ray sources (small triangles). They are spread across the FOV much more uniformly than either optical stars in cluster locus (Figure 10*a*) or the bulk of X-ray sources (Figure 7*a*), with at most a moderate clustering towards the center (partly caused by the lower on-axis detection threshold). This hard-source population appears to be different from (most of) the cluster population; since a subset of these hard sources probably belongs to the cluster, this "cloud-embedded" population appears to be less concentrated than the exposed part of the cluster, and may constitute another step in the star-formation sequence in this region.

Four hard X-ray sources have enough counts for a spectral analysis (see Paper II), and in all cases the best-fit absorption is found to be $\log N_H = 22.7 - 22.8$ (cm^{-2}), more than ten times the absorption of most cluster X-ray sources.

Our X-ray data alone are insufficient to study this embedded population in greater detail. Deep IR images, which will also permit the study of objects in the interior of the cloud or beyond it, would probably contribute significantly to this. A comparison of this hard-source population with the recently released 2MASS IR data will be given in Paper II.

Only two objects (in the southeast, neither optically identified) are common to both the hard-source and the X-ray flaring samples, indicating that these hard X-ray sources are no more eruptive than cluster stars.

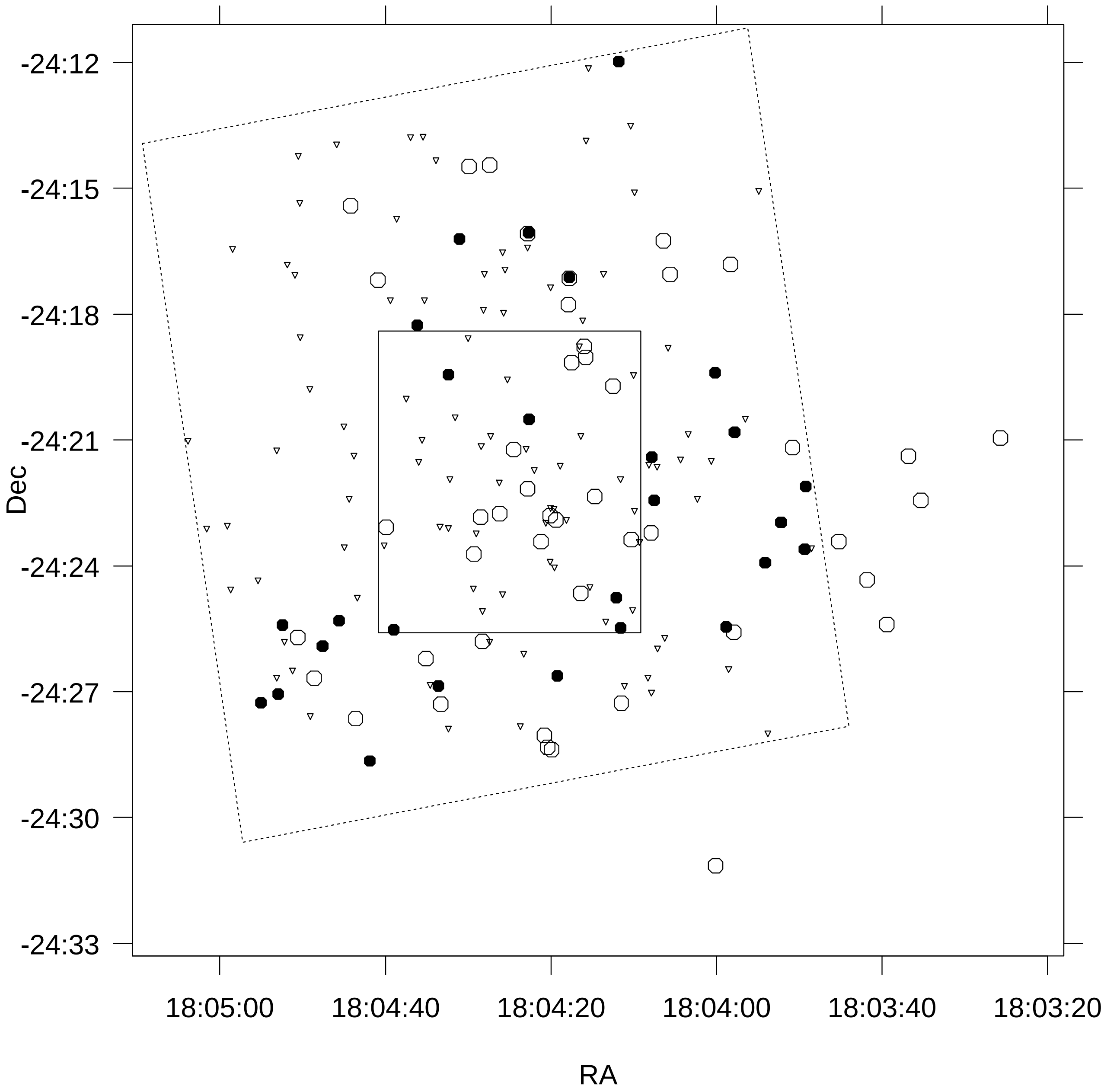

Fig. 16.— Spatial distribution of X-ray sources showing flares (filled circles), having a different spatial distribution than the bulk of X-ray detected sources (Figure 7*a*), but very similar to the distribution of very young cluster stars shown in Figure 13. Empty circles are Hα excess stars, having a more uniform distribution across the cluster. Small triangles indicate hard X-ray sources. Their space distribution is more uniform compared with the "cluster locus" distribution of Figure 10*a*.

5. Discussion

With a single deep, high-resolution *Chandra* X-ray observation of NGC 6530 we have gained a large amount of information on the stellar population of the cluster. Perhaps the single most important result is that NGC 6530 contains a population of at least 800 low-mass PMS stars; a deeper X-ray study would probably find more. Most of these low-mass stars have escaped all previous studies: only a few tens were previously known as either Hα emitters or variable stars. Our X-ray observation is so deep that about 3/4 of the detected X-ray sources have counterparts fainter than the $V = 17$ limit of the deepest available catalog of NGC 6530 optical stars by SCB. Even within this magnitude limit, our X-ray data have permitted the selection of about 180 PMS cluster members, compared with the 46 PMS members from the Hα study of SCB. *Chandra* X-ray observations have therefore proven to be by far the most efficient way to select low-mass PMS stars in a massive and distant (1800 pc) cluster such as NGC 6530. There is some complementarity between X-ray and Hα selection, since the strongest Hα emitters are not detected in X-rays, but the largest PMS samples cannot be selected in an Hα survey such as that of SCB.

As a consequence, the NGC 6530 initial mass function (IMF) in the low-mass range, previously derived mostly from Hα studies (SCB), must be taken with caution. There are far more low-mass stars than found by SCB, and while they estimated that the Hα selection completeness was about 50%, our new data show it is only half that value (at most) down to $V = 17$. Moreover, this value likely depends on the particular star-forming region and on the optical survey limit, since a value close to 50% was found in NGC 2264 by Flaccomio et al. (2000). Therefore, an extrapolation of results from Hα studies is unreliable, while a much more complete study is possible using X-ray selection of members. For NGC 6530 X-ray selected PMS stars we have a rather limited and age-dependent mass completeness (cf. § 4.5), due to the optical catalog used, and therefore we have not attempted to derive the cluster IMF in this work. This will be done in a forthcoming paper on the basis of deeper optical photometry (L. Prisinzano et al., in preparation).

In addition to deeper optical photometry, many data are still missing for a more complete knowledge of the stellar census of NGC 6530: deep Hα surveys, which have the potential of discovering X-ray undetected cluster stars, Lithium abundance and radial velocity surveys, capable of selecting members independently of their X-ray or Hα emission. To date, only the brighter cluster members have a spectroscopically determined spectral type. Also a deeper study of the existing 2MASS data on NGC 6530 will probably yield important insights on the cluster population and its evolution.

Another important result of the present study is the apparent presence of an age gradient across NGC 6530, with an older and more exposed region in the northwest contrasting with a younger, more embedded region in the south and southwest. This supports the idea of sequential formation, already proposed for the NGC 6530 region by Lada et al. (1976), although with a different pattern. In such a sequence, the bulk of NGC 6530 stars (including most bright stars) is found at intermediate ages, in the central cluster region, suggesting that star formation proceeds slowly at the beginning, then reaches a maximum rate, and declines afterwards, spreading to outer cloud regions, possibly triggered by the momentum injected in the cloud medium by the massive stars just formed in the cluster. A more detailed study requires deeper photometry to allow the placement on the H-R diagram of a larger number of X-ray selected cluster members.

This picture resembles qualitatively that proposed recently by Palla and Stahler (2002) for star formation in the Taurus region, despite differences between these clusters (in density and number of stars), and the different quality of the available data.

It is also interesting to study the (projected) speed at which the disturbance that has caused the sequence of star-formation events in NGC 6530 has progressed through the cloud medium. There is probably a formation sequence from cluster center towards southeast and southwest, where the youngest stars are found, but since very young stars are found in the central region as well, it is difficult to assign an age difference between these subgroups. A clearer view is instead obtained by comparing the distinctly different southeast and northwest regions, respectively. These two groups of stars, with typical ages of $\sim$ 0.5 Myr and $\sim$ 1.5 Myr, respectively, lie about $15'$ apart from one another. At the cluster distance (1800 pc), this distance is equivalent to 7.85 pc. Therefore, the disturbance speed is 7.85 pc/Myr, or 7.5 km/sec. This is much higher than the sound speed in a cold molecular cloud, but is comparable to the sound speed in a hotter H_{II} region (e.g., Spitzer 1978) such as M8, where NGC 6530 is found immersed. A lower speed for the disturbance in the primordial NGC 6530 when neither massive stars nor the H_{II} region had yet formed, may explain why star formation proceeded more slowly at the beginning. All things considered, it is hardly surprising to find a non-simultaneous star formation over such a large region as NGC 6530. At least, one would expect a center-to-border age gradient, as is found in the Orion Nebula (unless an unknown large-scale synchronization mechanism were operating).

It is also interesting to note the similarity of this disturbance speed just derived with the results presented by Lada et al. (1976), namely that the M8 H_{II} region is moving towards the observer relative to the background molecular (CO) cloud at a relative speed of 7 km/sec, nearly the same as our value (which however refers to the transverse direction). Moreover, the Lada et al. CO "Bright Spot 3" is nearly coincident with the NGC 6530 cluster, and across it they observe a radial-velocity gradient of ^{12}CO along north-south: the southern emission is blue-shifted with respect to cluster center by $\sim$ 5 km/sec, and they note that it is difficult to interpret this as coherent cloud motion. This, together with our previous findings, suggests that the "disturbance" triggering star formation in NGC 6530 is not like a shock/sound wave in a static medium, but is more probably an expansion of part of the molecular cloud with respect to another, more dense, cold and massive part.

6. Summary

We have made a deep X-ray study of the very young cluster NGC 6530 using the *Chandra* ACIS. Our main results include the following:

- We have detected 884 point X-ray sources, strongly clustered around the NGC 6530 center, and argue that more than 800 of them are cluster members, a significant increase in the known NGC 6530 population at low and intermediate masses;

- The optical counterparts of these X-ray sources are found in a band in the H-R diagram, lying above the main sequence at the cluster distance, and coincident with the predicted locus of 0.5-1.5 Myr pre-main-sequence stars, mostly of low mass down to 0.5-1.5$M_{\odot}$;

- Although three-quarters of the total X-ray detections are yet to be identified optically, we argue that they are probably lower-mass cluster members. This is supported also by the 2MASS identification, available for 731 X-ray sources;

- Finding an age difference between cluster stars in the northwest and those in the south of the observed region, we propose that sequential formation has occurred in NGC 6530;

- We find that X-ray and Hα selection criteria are complementary, but the completeness of X-ray selection is much larger than that of Hα selection in NGC 6530;

- We find a number of flaring X-ray sources whose spatial distribution suggests extremely young ages and supports an age difference across the cluster;

- We find a population of hard X-ray sources, which may be either background objects and/or a more embedded cluster population;

We wish to thank the referee, Marc Gagné, for his stimulating comments and suggestions. This study has made use of data from the SIMBAD database, operated at the Centre de Données Astronomiques, Strasbourg. F.D., E.F., G.M., and S.S. acknowledge support from the Italian ASI and MIUR. SSM and FRH gratefully acknowledge partial support of NASA Contract NAS8-38248.

REFERENCES

Allen, C. W. 1973, Astrophysical quantities, 3rd ed., Athlone Press

Chini, R. & Neckel, T. 1981, A&A, 102, 171

Cutri, R. M., et al. 2003, Explanatory Supplement to the 2MASS All Sky Data Release, http://www.ipac.caltech.edu/2mass/releases/allsky/doc/explsup.html

Damiani,F., Maggio,A., Micela,G., and Sciortino,S. 1997a, ApJ, 483, 350

Damiani,F., Maggio,A., Micela,G., and Sciortino,S. 1997b, ApJ, 483, 370

Damiani,F., Flaccomio,E., Micela,G., Sciortino,S., Harnden,F.R., Murray,S.S., Wolk,S.J., Jeffries,R.D. 2003, ApJ, 588, in press

Ebisawa, K., Maeda, Y., Kaneda, H., Yamauchi, S. 2001, Science, 293, 1633

Feigelson, E. D., Broos, P., Gaffney, J. A., Garmire, G., Hillenbrand, L. A., Pravdo, S. H., Townsley, L., & Tsuboi, Y. 2002, ApJ, 574, 258

Flaccomio, E., Micela, G., Sciortino, S., Damiani, F., Favata, F., Harnden, F. R., & Schachter, J. 2000, A&A, 355, 651

Flaccomio, E., Damiani, F., Micela, G., Sciortino, S., Harnden, F. R., Murray, S. S., & Wolk, S. J. 2003a, ApJ, 582, 382

Flaccomio, E., Damiani, F., Micela, G., Sciortino, S., Harnden, F. R., Murray, S. S., & Wolk, S. J. 2003b, ApJ, 582, 398

Harnden, F. R. et al. 2001, ApJ, 547, L141

Hillenbrand, L. A. 1997, AJ, 113, 1733

Kholopov, P. N. et al. 1998, Combined General Catalogue of Variable Stars, 4.1 Ed. (1998)

Kilambi, G. C. 1977, MNRAS, 178, 423

Lada, C. J., Gottlieb, C. A., Gottlieb, E. W., & Gull, T. R. 1976, ApJ, 203, 159

Palla, F. & Stahler, S. W. 2002, ApJ, 581, 1194

Rauw, G., Nazé, Y., Gosset, E., Stevens, I. R., Blomme, R., Corcoran, M. F., Pittard, J. M., & Runacres, M. C. 2002, A&A, 395, 499

Rieke, G. H. & Lebofsky, M. J. 1985, ApJ, 288, 618

Sagar, R. & Joshi, U. C. 1978, MNRAS, 184, 467

Siess, L., Dufour, E., & Forestini, M. 2000, A&A, 358, 593

Simon, M., Dutrey, A., & Guilloteau, S. 2000, ApJ, 545, 1034

Spitzer, L. 1978, Physical Processes in the Interstellar Medium, Wiley

Sung, H., Bessell, M. S., & Lee, S. 1998, AJ, 115, 734

Sung, H., Chun, M., & Bessell, M. S. 2000, AJ, 120, 333 (SCB)

The, P. 1960, ApJ, 132, 40

Tothill, N. F. H., White, G. J., Matthews, H. E., McCutcheon, W. H., McCaughrean, M. J., & Kenworthy, M. A. 2002, ApJ, 580, 285

Townsley, L. K., Broos, P. S., Garmire, G. P., & Nousek, J. A. 2000, ApJ, 534, L139

van Altena, W. F. & Jones, B. F. 1972, A&A, 20, 425

van den Ancker, M. E., The, P. S., Feinstein, A., Vazquez, R. A., de Winter, D., & Perez, M. R. 1997, A&AS, 123, 63

Walker, M. F. 1957, ApJ, 125, 636

Weisskopf, M. C., Brinkman, B., Canizares, C., Garmire, G., Murray, S., & Van Speybroeck, L. P. 2002, PASP, 114, 1

This preprint was prepared with the AAS LATEX macros v5.0.